Polar winter climate change: strong local effects from sea ice loss, widespread consequences from warming seas

Tuomas Naakka[1], Daniel Köhler[2], Kalle Nordling[3,4], Petri Räisänen[3], Marianne Tronstad Lund[4], Risto Makkonen[2,3], Joonas Merikanto[3], Bjørn H. Samset[4], Victoria A. Sinclair[2], Jennie L. Thomas[5], Annica M. L. Ekman[1]

[1]Department of Meteorology and Bolin Centre for Climate Research, Stockholm University, Stockholm, Sweden.
[2]Institute for Atmospheric and Earth System Research/Physics, Faculty of Science, University of Helsinki, Helsinki, Finland
[3]Finnish Meteorological Institute, Helsinki, Finland
[4]CICERO Center for International Climate Research, Oslo, Norway
[5]Univ. Grenoble Alpes, CNRS, INRAE, IRD, Grenoble INP, IGE, 38000 Grenoble, France

Correspondence to: Annica Ekman (annica.ekman@misu.su.se)

Abstract. Decreasing sea ice cover and warming sea surface temperatures (SSTs) impact ~~polar~~ climate at both poles in uncertain ways. We aim to reduce the uncertainty by comparing output from four 41-year simulations with four Atmospheric General Circulation Models (AGCMs). In our baseline simulations, the models use identical prescribed SSTs and sea ice cover conditions representative of 1950-1969. In three sensitivity experiments, the SSTs and sea ice cover are individually and simultaneously changed to conditions representative of 2080-2099 in a strong warming scenario. Overall, the models agree that warmer SSTs have a widespread impact on 2m temperature and precipitation while decreasing sea ice cover mainly causes a local response (i.e. the largest ~~effect~~ warming occurs where ~~the~~ sea ice ~~perturbation occurs~~ is perturbed). Thus, decreasing sea ice cover causes ~~a~~ larger change~~s~~ in precipitation and temperature than warmer SSTs in areas where sea ice cover is reduced while warmer SSTs dominate the response elsewhere. In general, the response in temperature and precipitation to simultaneous changes in SSTs and sea ice cover is approximately equal to the sum due to individual changes, except in areas of sea ice decrease where the joint effect is smaller than the sum of the individual effects. The models agree less well on the magnitude and spatial distribution of the response in mean sea level pressure, i.e. uncertainties associated with atmospheric circulation responses are larger than uncertainties associated with thermodynamic responses. Furthermore, the circulation response to decreasing sea ice cover is sometimes significantly enhanced but sometimes counteracted by the response to warmer SSTs.

Short summary. The effects on polar climates of warmer sea surface temperatures and decreasing sea ice cover have been studied using four climate models with identical prescribed changes in sea surface temperatures and sea ice cover. The models predict similar changes in air temperature and precipitation in the polar regions in a warmer climate with less sea ice. However, the models disagree on how the atmospheric circulation, i.e. the large-scale winds, will change with warmer temperatures and less sea ice.

1. Introduction

Dramatic sea ice loss has been recorded at both poles during the last decade (Parkinson, 2019; Parkinson, 2022). The reduction in sea ice is most pronounced in the Arctic, where the surface has warmed nearly four times faster than the global average over the past forty-five years (Rantanen et al., 2022). The rate and magnitude of sea ice loss are projected to continue at both poles – they may even increase if there are no drastic cuts in greenhouse emissions (IPCC, 2022). This transition in polar climates can potentially affect weather patterns across the whole globe (Cohen et al., 2014; Vihma, 2014; England et al., 2020; Tewari et al., 2023) and will without a doubt have large consequences for people living within or near the polar regions.

Earth System Models (ESMs) as well as Atmospheric General Circulation Models (AGCMs) agree on many general features of a warmer future Arctic and Antarctic, but they strongly disagree on critical details, such as the exact magnitude of the warming and sea ice reduction rates (Stuecker et al., 2018; Han et al., 2023). These discrepancies may influence our understanding of how changes in sea ice affect circulation patterns and weather systems within and outside the polar regions (Smith et al., 2022). Polar warming rates depend on local feedback processes (e.g. changes in clouds, precipitation, sea ice extent) as well as changes in remote drivers (e.g. oceanic and atmospheric heat transport), which both are highly uncertain (Lenaerts et al., 2017; Wendish et al., 2019; Kim and Kim, 2018; Cronin et al., 2017). Several studies have pointed out the importance of better understanding local feedbacks in polar regions, in particular related to clouds, for better constraining the magnitude of polar amplification and ice melt (Screen et al., 2018; Kittel et al., 2022; Ryan et al., 2022).

To address the issues outlined above, we have designed and executed a set of coordinated simulations with four different AGCMs. The idealized simulations have been performed with individual and simultaneous changes in prescribed sea surface temperatures (SSTs) and sea ice cover following a future anthropogenic emission scenario. The experimental setup allows us to isolate feedbacks that are driven either by SST or sea ice cover changes, and to examine the linearity of these feedbacks. Using four different AGCMs, we can also investigate the robustness of the atmospheric responses. The overall aim has been to better understand the processes that drive interactions between polar regions and lower latitudes, their structural uncertainty, and their response to local and remote forcing under changing climate conditions. An additional aim is to contribute to model development as the results are dependent on the ability of the models to describe atmospheric processes. In this paper, we describe the simulation setup and discuss some high-level results with a focus on basic meteorological variables (two-meter air temperature, surface precipitation, and mean sea level pressure).

Specifically, we target the following questions:
- When models are constrained by prescribed SSTs and sea ice cover changes, do they agree on how basic meteorological parameters in the polar regions change in a warmer climate?

65 ● How large are inter-model differences in the simulated responses in, on one hand, thermodynamic quantities like air
66 temperature, and on the other hand, dynamic quantities like mean sea-level pressure?
67 ● What is the most important oceanic driver of the atmospheric responses within the polar regions and in mid-latitudes,
68 changes in SST or sea ice cover?
69 Our analysis is focused on the winter season in the Arctic and Antarctic, when changes in atmospheric circulation patterns
70 should be most prominent and the decrease in sea ice cover has the most notable impact on meteorological variables (e.g.
71 Screen and Simmonds 2010).
72

2. Methods

2.1 Experimental setup

75 A Baseline simulation and three different perturbation experiments from four different AGCMs (see Section 2.2) were
76 performed and analyzed (Table 1). The experiments follow an Atmospheric Model Intercomparison Project (AMIP)
77 configuration (Gates, 1992; Gates et al., 1999). In all experiments, we used prescribed SSTs (variable "tos") and sea ice area
78 fraction (variable "siconc", hereafter referred to as "sea ice cover") from simulations with the Australian Earth system model
79 ACCESS-ESM1.5 (Ziehn et al., 2020; Ziehn et al., 2019a,b) available from the Coupled Model Intercomparison phase 6
80 (CMIP6) archive. We chose ACCESS-ESM1.5 output for our simulations as the model produces an Arctic sea ice cover
81 evolution for the historical period that is in reasonable agreement with observations (Notz et al., 2020). The model was also
82 selected by the CMIP6 Sea-Ice Model Intercomparison Project community to estimate a best guess of the future evolution of
83 Arctic sea ice cover (Notz et al., 2020). Monthly-mean SST and sea ice cover averaged over 20 years of simulation were taken
84 from either the historical simulation (years 1950-1969, Baseline simulation), or the scenario SSP5-8.5 simulation (years 2080-
85 2099), and the same annual cycle was repeated for the whole 41-year simulations. A similar set of model runs was performed
86 for the low-emissions SSP1-2.6 scenario, but in the interest of brevity, only the SSP5-8.5 results are discussed in this paper.
87 In addition, the large changes in sea ice cover and SST in the SSP5-8.5 scenario amplify the effects of warming and thus the
88 SSP5-8.5 simulation makes the signal-to-noise ratio significantly stronger than in the SSP1-2.6 scenario. SSTs and sea ice
89 cover were linearly interpolated between each month and changed both individually and simultaneously compared to the
90 Baseline simulation (Table 1). Note that our experimental setup is different to e.g. the Polar Amplification Model
91 Intercomparison Project (PAMIP, Smith et al., 2019). In the PAMIP experiments, mostly short (1 year) simulations were
92 performed with large ensembles of initial states, whereas our experiments consist of long (40 years) simulations. The PAMIP
93 simulations address pre-industrial, present-day and future climates, whereas our simulations focus only on differences between
94 present-day and future climates. The changes in sea ice cover and SSTs were also substantially larger in our experiments than
95 in the PAMIP atmosphere-only simulations. In ACCESS-ESM1.5 i.e. the model we use for the SST and sea ice forcing fields,
96 the global average increase in 2m temperature between the baseline and future period (using the SSP 5-8.5 scenario) is 4.4 K,

3

97 whereas the warming in the PAMIP simulations warming is approximately 2 K comparing future and pre-industrial conditions.

98 In our future simulations, the Arctic Ocean is almost ice-free during the whole year (Fig. 1), which. ~~In addition, the PAMIP~~

99 ~~experiments were designed to study causes and consequences of Arctic amplification in present day climate, while our~~

100 ~~simulation setup is aimed at a future warmer climate. Furthermore, we examined the multi-model response to changes in~~

101 ~~prescribed SSTs and sea ice cover without any influence from model-specific differences in these variables (and thus with a~~

102 ~~small influence of the individual internal climate variability of each model). The scenario chosen is representative of a high~~

103 ~~(SSP5-8.5) future warming. Accordingly, differences in SST and sea ice cover between the SSP5-8.5 and the Baseline~~

104 ~~conditions are large, with an almost ice free Arctic Ocean during the whole year (Fig. 1).~~ helps to boost the signal-to-noise

105 ratio of the simulated climate responses. Another difference compared to the PAMIP experiments is that our forcing fields are

106 only based on output from one model (ACCESS-ESM1.5) whereas PAMIP uses a combination of observations and multi-

107 model averages.

108

109 **Table 1. Name of model experiments and their respective SST and sea ice cover configuration.**

	Historical sea ice	SSP5-8.5 sea ice
Historical SST	Baseline	SIC_SSP585
SSP5-8.5 SST	SST_SSP585	SSP585

110

111

112

113 Each experiment was run for 41 years, with perpetual monthly average values of SSTs and sea ice cover. All other conditions

114 (e.g. greenhouse gas concentrations, aerosol emissions etc.) were prescribed according to the year 2000 in all models and

115 experiments. Each model used their default parameterizations of snow and ice albedos as well as for natural aerosols (see

116 Section 2.2). The first year of simulation was considered as a spin-up and discarded from the analysis, leaving 40 years of

117 output for analysis. In the simulations where only the sea ice cover was changed (i.e. SIC_SSP585), the SSTs were kept at

118 their Baseline values. This means that the surface temperature is reduced slightly over areas where sea ice is removed since

119 the temperature of the sea-ice - ocean-water interface is slightly lower than the melting point of freshwater. Based on our

120 simulations, the total climate response (ΔX_{full}) for any given variable caused by the use of future boundary conditions (SSP5-

121 8.5) compared to Baseline can be decomposed into three parts:

122

123 $$\Delta X_{full} = \Delta X_{SST} + \Delta X_{SIC} + \Delta X_{NL} \hspace{3cm} (1)$$
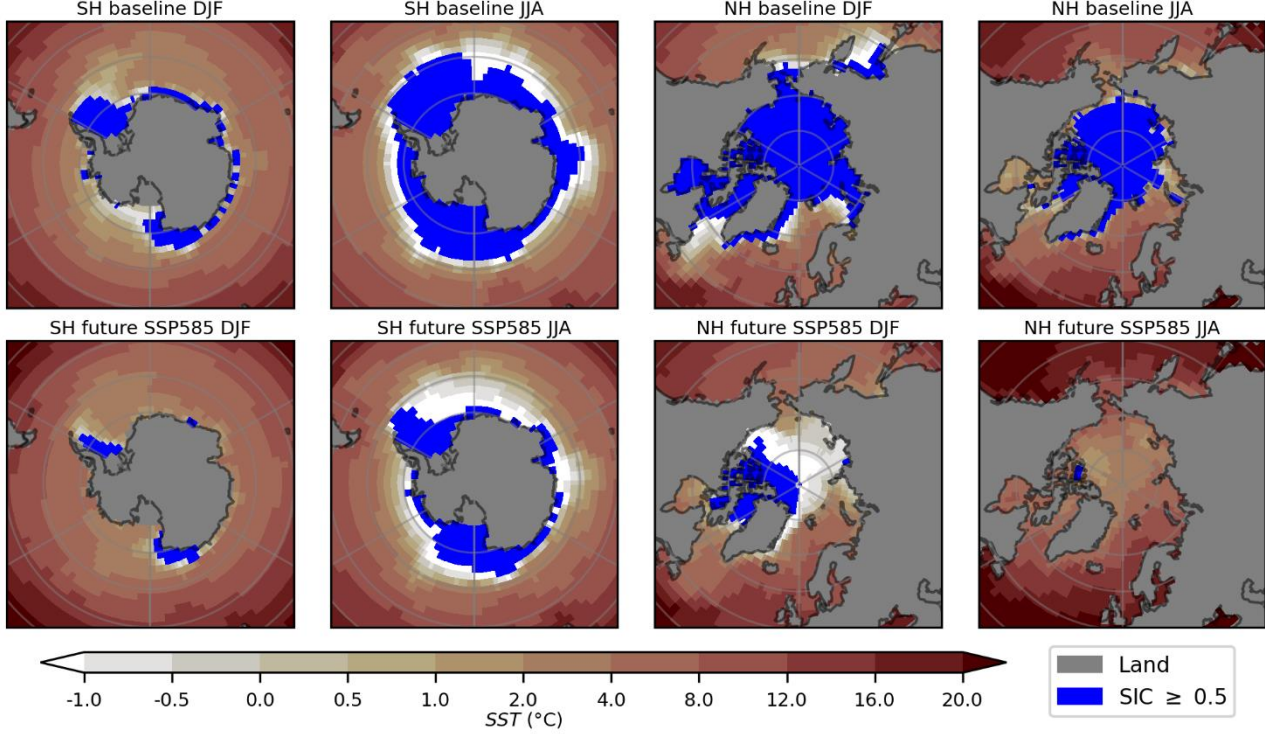
124

125 where X is any climate variable (e.g. temperature or precipitation) and ΔX_{SST} is the contribution from the SST change, ΔX_{SIC} is

126 the contribution from the sea ice cover change, and ΔX_{NL} is the nonlinear (or residual) contribution:

4

127

$$\Delta X_{full} = X_{SSP585} - X_{Baseline} \qquad (2)$$

$$\Delta X_{SST} = X_{SST\ SSP585} - X_{Baseline} \qquad (3)$$

$$\Delta X_{SIC} = X_{SIC\ SSP585} - X_{Baseline} \qquad (4)$$

$$\Delta X_{NL} = \Delta X_{full} - \Delta X_{SST} - \Delta X_{SIC} \qquad (5)$$

Figure 1: Winter (DJF) and summer (JJA) mean sea ice cover and sea surface temperature (SST) in the Baseline experiment (upper row), and in the SSP585 experiment (lower row).

2.2 Models

Three ESMs (CESM2, NorESM2, and EC-Earth3) and one AGCM (OpenIFS) were used in the study. The selection of models allows us to compare differences between models belonging to the same as well as different model families. CESM2 and NorESM2 are based on the same dynamical core but differ for some parametrizations of physical processes. Similarly, EC-Earth3 and OpenIFS belong to the same model family. Our model selection also is affected by the fact the study is part of the CRiceS-project (Climate Relevant interactions and feedbacks: The key role of sea ice and Snow in the polar and global climate system) which aims to improve the description of polar atmospheric processes in ESMs, in particular NorESM2 and EC-Earth3. Below we provide a brief description of the models.~~three ESMs (CESM2, NorESM2, and EC-Earth3) and the AGCM (OpenIFS) used in the study.~~ We only describe the atmospheric part of each model since we use prescribed SSTs and sea ice cover in all simulations. Note that the different model components were connected to each other through heat, radiative, and

5

145 momentum fluxes during the simulations, but the ocean and sea ice components were not utilized for predicting the evolution

146 of sea ice or SSTs (since these were prescribed in the experiments). In other words, the sea ice model was only utilized to

147 compute e.g. the surface temperature of sea ice and the surface fluxes between the atmosphere and sea ice. The surface albedo,

148 including the effects of snow, was computed within the sea ice and land components.

2.2.1 CESM2

150 The atmospheric component of the community Earth system model version 2 (CESM2) is the Community Atmosphere Model

151 version 6 (CAM6, Danabasoglu et al., 2020). CAM6 is based on a hydrostatic finite-volume dynamical core with a regular

152 latitude–longitude grid. The horizontal resolution of CAM6 is $1.25° \times 0.9°$ (lon $\times$ lat) and the model has 32 vertical levels up

153 to 2.3 hPa. The aerosol module is the Modal Aerosol Model version 4 (MAM4, Liu et al., 2016) and aerosols are interactive

154 with clouds. Radiative transfer is modelled using the Rapid Radiative Transfer Model for General circulation models, RRTMG

155 (Danabasoglu et al., 2020). Cloud microphysics follows a two-moment scheme with four hydrometeor species (cloud water,

156 cloud ice, rain, and snow) (Gettelman and Morrison, 2015) and mixed phase clouds can occur in the temperature range 0 to -

157 37°C (Gettelman et al., 2010). The other model components in CESM2 are the Community Land Model 5.0 (CLM5) for land

158 processes and interactions between the land and atmosphere, the Model for Scale Adaptive River Transport (MOSART) for

159 river runoff, the Community Ice CodE (CICE) for sea ice, SWAV for oceanic waves and the Community Ice Sheet Model

160 (CISM) for land ice.

2.2.2 NorESM2

162 The Norwegian Earth System Model version 2 (NorESM2, Seland et al., 2020) originates from CESM2. NorESM2 thus has

163 many model components that are the same as in CESM2. The main difference is that CAM6 has been replaced by CAM6-Nor.

164 In addition, the land ice and ocean wave components have not been used in the NorESM2 experiments. CAM6-Nor uses the

165 same cloud and radiation schemes as CAM6. The largest differences between CAM6 and CAM6-Nor are associated with the

166 aerosol physics and aerosol-cloud-radiation interactions (Seland et al., 2020, Kirkevåg et al., 2013, 2018). For the current

167 study, we use the low-resolution model version of NorESM2, which has a horizontal resolution of $2.5° \times 1.9°$ (lon $\times$ lat) and

168 the same vertical levels as CESM2.

169

170 The evolution of different aerosol particle types is described with the NorESM2 aerosol scheme. Aerosol particles interact

171 with clouds affecting e.g. cloud droplet activation and freezing of cloud droplets (Storelvmo et al., 2006). Formation of ice

172 crystals may occur due to heterogeneous nucleation and heterogeneous freezing where mineral dust and black carbon can act

173 as ice nucleating particles (Kirkevåg et al., 2018).

2.2.3 OpenIFS

OpenIFS is a research model built from the Integrated Forecast System (IFS), the operational numerical weather prediction (NWP) model from the European Center for Medium-Range Forecasts (ECMWF). We have used the version 43r3 of OpenIFS (hereafter referred to as OpenIFS), which is derived from IFS CY43R3 (used for operational forecasting at ECMWF from July 2017 to June 2018). The dynamical core uses spectral semi-Lagrangian and semi-implicit methods. The experiment configuration uses spectral linear truncation TL255 (approx. 80 km at the equator) as horizontal resolution and 91 hybrid model levels up to 0.01hPa.

The version of OpenIFS used does not include interactive aerosols. The radiation scheme uses global aerosol fields from monthly climatological means produced by the Copernicus Atmospheric Monitoring Service. Cloud condensation nuclei concentrations are prescribed as one constant value over land and ocean, respectively. The exact implementation is described in Bozzo et al. (2017).

OpenIFS 1-moment cloud scheme contains 6 moisture related prognostic variables (water vapor, cloud water, cloud ice, cloud fraction, rain, and snow). The prognostic cloud fraction and sources and sinks for cloud variables are calculated from the major generation and destruction processes. The separate treatment for cloud water and cloud ice allows for the representation of supercooled liquid and mixed phase clouds. (ECMWF: IFS Documentation CY43R3). The radiation processes of OpenIFS 43r3 are handled by the ecRad scheme (Hogan and Bozzo, 2018).

The land surface scheme in OpenIFS is handled by the Hydrology Tiled ECMWF Scheme for Surface Exchanges over Land (HTESSEL) (Balsamo et al. 2009), which also handles surface fluxes due to sea surface temperature and sea ice, which are controlled by the experiments described above. Furthermore, OpenIFS includes an ocean surface wave model, which couples the wind wave interaction and calculates the kinematic part of the energy balance equation over the ocean.

OpenIFS is primarily intended as a model for NWP. Nevertheless, configurations for nudged or free-run simulation are implemented. The free-run configuration has been used in the present study, in tandem with in-build fixers for global mass and moisture to produce atmosphere-only climate simulation.

2.2.4 EC-Earth3

The EC-Earth3 experiments were carried out with EC-Earth3-AerChem version 3.3.4.1 (van Noije et al., 2021, Döscher at al. 2022), which is the model configuration with interactive aerosols and atmospheric chemistry used in the Aerosol and Chemistry Model Intercomparison Project (AerChemMIP). The atmospheric component of EC-Earth3 is based on the ECMWF IFS

206 CY36R4, which was operational from November 2010 to May 2011. Land surface processes are simulated with HTESSEL.

207 The cloud scheme in EC-Earth3 is the same as in OpenIFS but there are differences in the treatment of other physical processes

208 including convection, and radiation is parameterized with the McRad scheme (Morcrette et al. 2008). Aerosols and chemical

209 processes in the atmosphere are described by the chemical transport model Tracer Model version 5 (TM5) (van Noije et al.,

210 2014). Tropospheric aerosols influence the cloud droplet number concentration but not the ice number concentrations. The

211 spatial discretization of the atmospheric model was the same as for OpenIFS, that is, TL255 in the horizontal and 91 levels in

212 the vertical, while TM5 was run at a lower resolution, $3° \times 2°$ (lon $\times$ lat) with 34 vertical levels and a top at 0.1 hPa.

3. Results

214 The experiments targeting our science questions were not covered by the CMIP6 protocol; therefore, we use the specific model

215 protocol defined in Section 2.1. Given this, our results cannot be directly compared with the historical and future scenario

216 (SSP5-8.5) simulations. Most importantly, we use prescribed SSTs and sea ice cover from one specific model (ACCESS-

217 ESM1.5) and we also apply constant greenhouse gas concentrations (for the year 2000) in all simulations. Nevertheless, in

218 Section 3.1 we compare our Baseline and SSP_585 experiments with the historical (years 1950-1969) and scenario SSP5-8.5

219 (years 2080-2099) experiments from CMIP6 to put our simulation results into the context of these simulations. In Sections 3.2

220 and 3.3 we thereafter examine the future climate response in the Antarctic and Arctic, respectively, by comparing our future

221 simulations (SSP585, SST_SSP585, SIC_SSP585) with Baseline (see Table 2). In the analysis, we focus on the winter seasons

222 in both hemispheres and start our analysis with the Antarctic region which has received less attention than the Arctic in previous

223 research.

3.1 Comparison with CMIP6 models

225 Figs. 2 and S1 shows that our Baseline and SSP585 simulations agree well with the corresponding CMIP6 simulations for

226 several key climate variables, even though the boundary conditions are slightly different. The simulated zonal mean 2m

227 temperature, mean sea level pressure (MSLP) and precipitation are within the range of the minimum and maximum of the 23

228 CMIP6 models and they are also generally close to the CMIP6 multi-model mean (Figures 2 and S1). This result indicates that

229 our simulations reproduce the general features of the historical and future (SSP5-8.5) climate conditions as modelled by

230 CMIP6.

231

232 In the Baseline simulation, the largest deviations from the CMIP6 multi-model mean 2m temperature occur at the winter poles,

233 where our models are generally warmer than the CMIP6 multi-model mean (Fig. 2a,d). This difference may be associated with

234 the different greenhouse gas and aerosol concentrations applied in the present study (which are from the year 2000). However,

235 the simulated 2m temperatures in our SSP585 simulations and the differences between our Baseline and SSP585 simulations

236 are in general close to the CMIP6 SSP5-8.5 multi-model mean and the differences between corresponding CMIP6 historical

and CMIP6 SSP5-8.5 simulations (Fig. S1 and S2), despite the differences in greenhouse gas and aerosol concentrations. The largest MSLP deviations from the CMIP6 multi-model mean also occur in the polar regions (Figs, 2b, e). In particular, CESM2 and NorESM2 have a deeper circumpolar trough and a stronger subtropical high over the southern hemisphere, suggesting stronger westerly winds over the Southern Ocean. In terms of precipitation, our model simulations agree well with the CMIP6 multi-model mean (Figs. 2c, f).
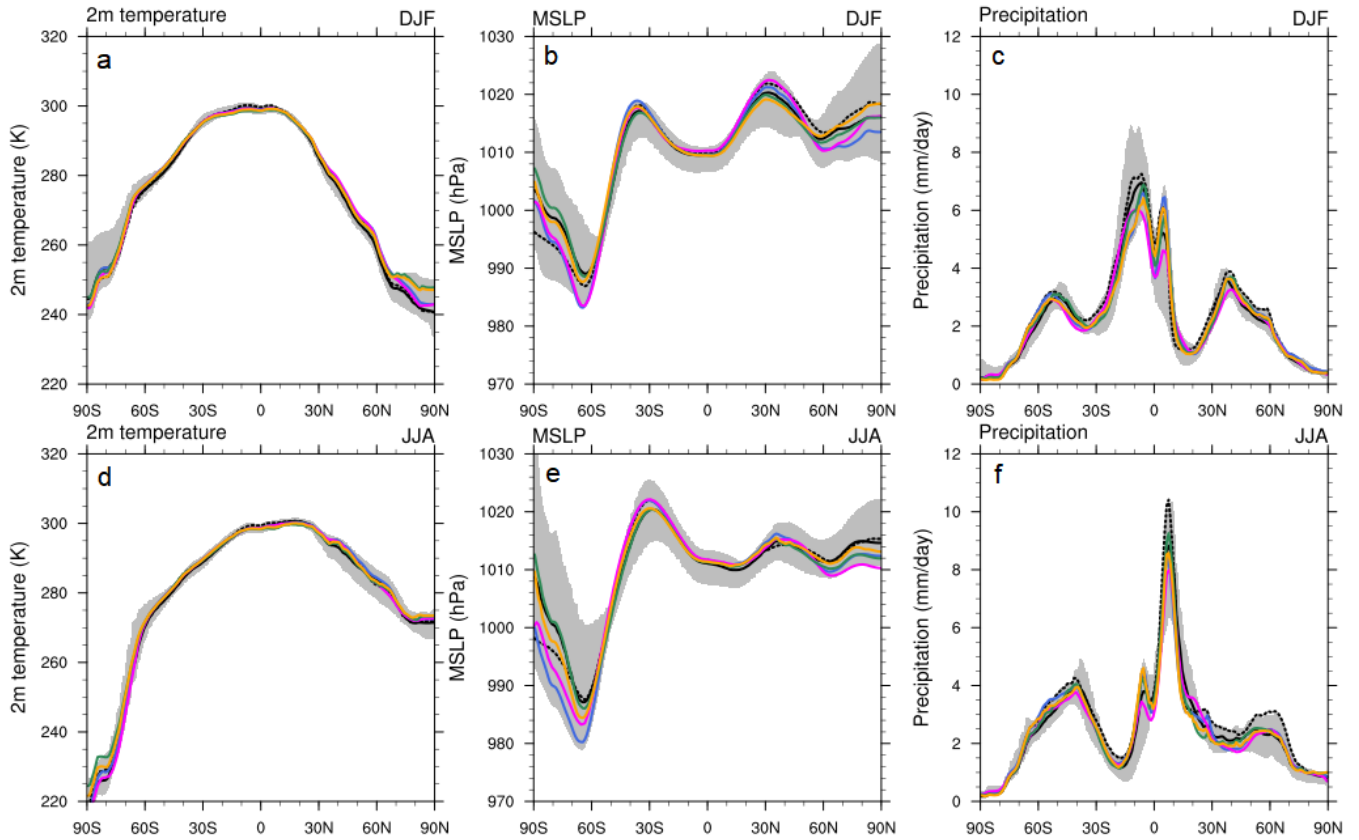

Figure 2. Seasonal means of zonal mean of 2m temperature (left, a, d), mean sea level pressure (middle, b, e), and precipitation (right, c, f), in the Baseline simulations and in the CMIP6 historical simulations (years 1950-1969). The blue (CESM2), magenta (NorESM2), green (EC-Earth3) and yellow (OpenIFS) lines show the models applied in the present study and the black solid line shows the CMIP6 multi-model mean and black dashed line shows ACCESS-ESM1.5 CMIP6 simulation where sea ice cover and SST were taken. The gray area shows the range between the minimum and maximum of the 23 CMIP6 models. The upper row shows mean values for northern hemisphere winter (DJF) and the lower row shows mean values for southern hemisphere winter (JJA).
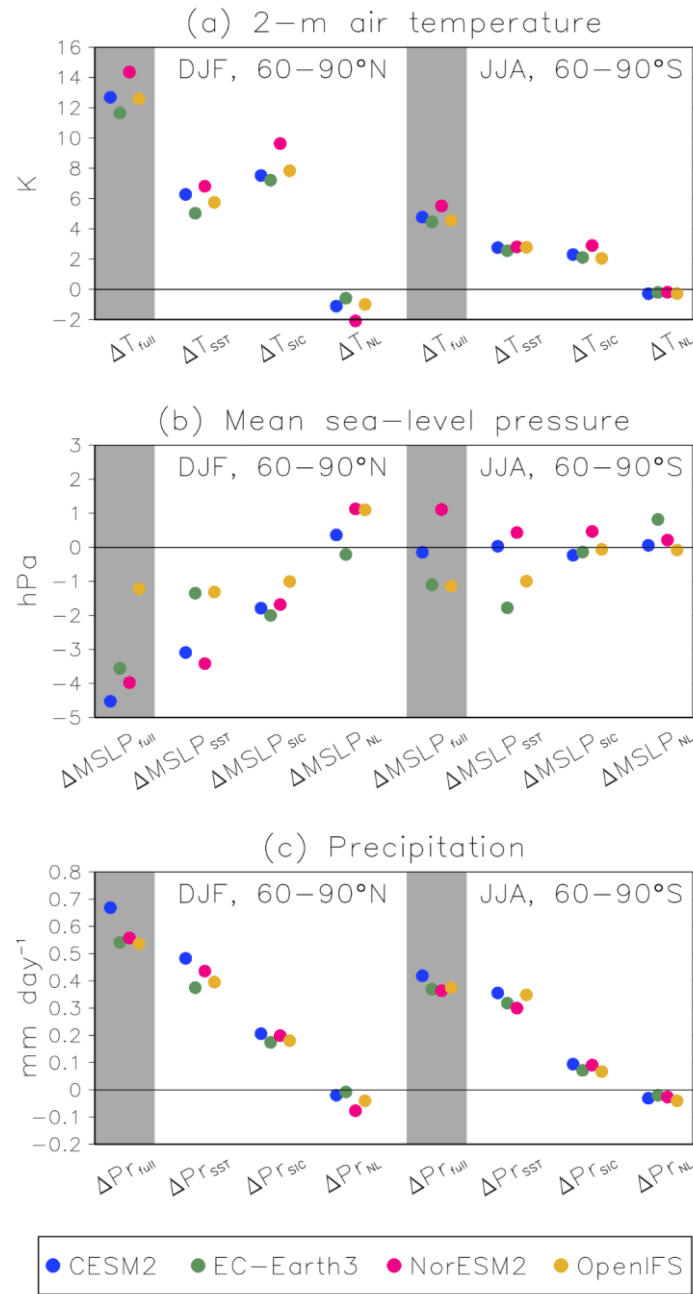
Figure 3. Area-mean differences between the SSP585 simulation and Baseline (ΔX_{full}, grey shading), between SIC_SSP585 and Baseline (ΔX_{SIC}), between SST_SSP585 and Baseline (ΔX_{SST}), and the nonlinear (residual) contribution (ΔX_{NL}) for (left) northern high latitudes (60-90°N) in the northern hemisphere winter (DJF) and (right) southern high latitudes (60-90°S) in the southern hemisphere winter(JJA) for (a) 2m temperature, (b) mean sea-level pressure, and (c) precipitation.

3.2 Antarctic

3.2.1 Temperature

As an ~~On~~ average over the Antarctic (60 - 90°), the models agree on the changes in 2m temperature ~~due~~both when SST and sea ice cover are changed jointly as well as ~~increase in SST and decreases in sea ice cover~~ when they are changed individually (Fig. 3a). The increase in SSTs and the decrease in sea ice cover cause on average an almost equal change in wintertime (JJA) 2m temperature in the southern polar region. ~~In the southern hemisphere winter (JJA), t~~The largest increase in 2m temperature between SSP585 and Baseline (ΔT_{full}) occurs over the Southern Ocean, around the Antarctic continent where the sea ice has been removed (up to 11K, Fig. 4a). The 2m temperature increases significantly also over the Antarctic continent, but the increase is smaller, mostly 4K - 5K. The models generally agree on the warming pattern (Fig. S3), but there are quantitative differences (Fig. 4e). These are in general spatially correlated with the strength of warming, except over the Weddell Sea, where the strongest warming over the Antarctic region occurs and the differences between the models are small.
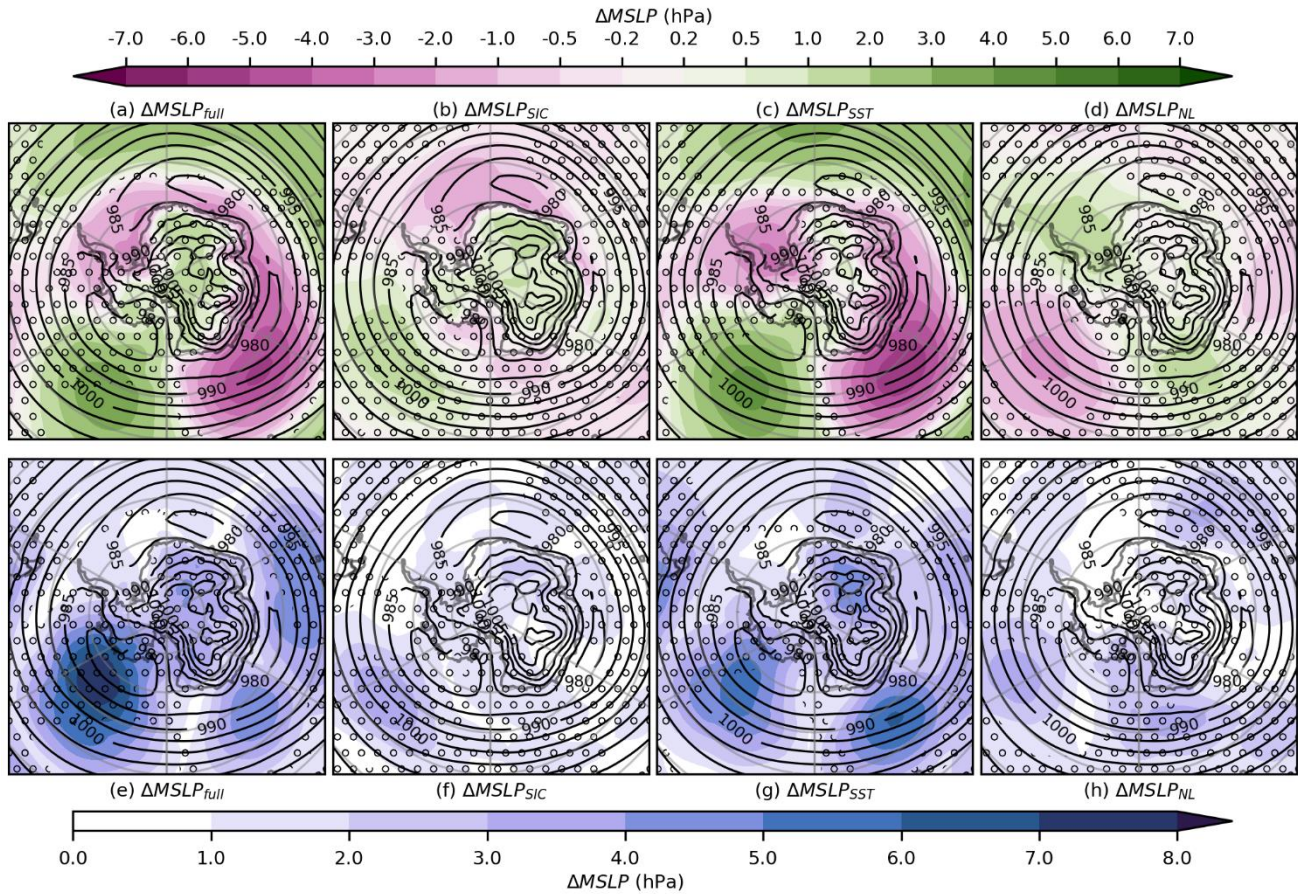

11
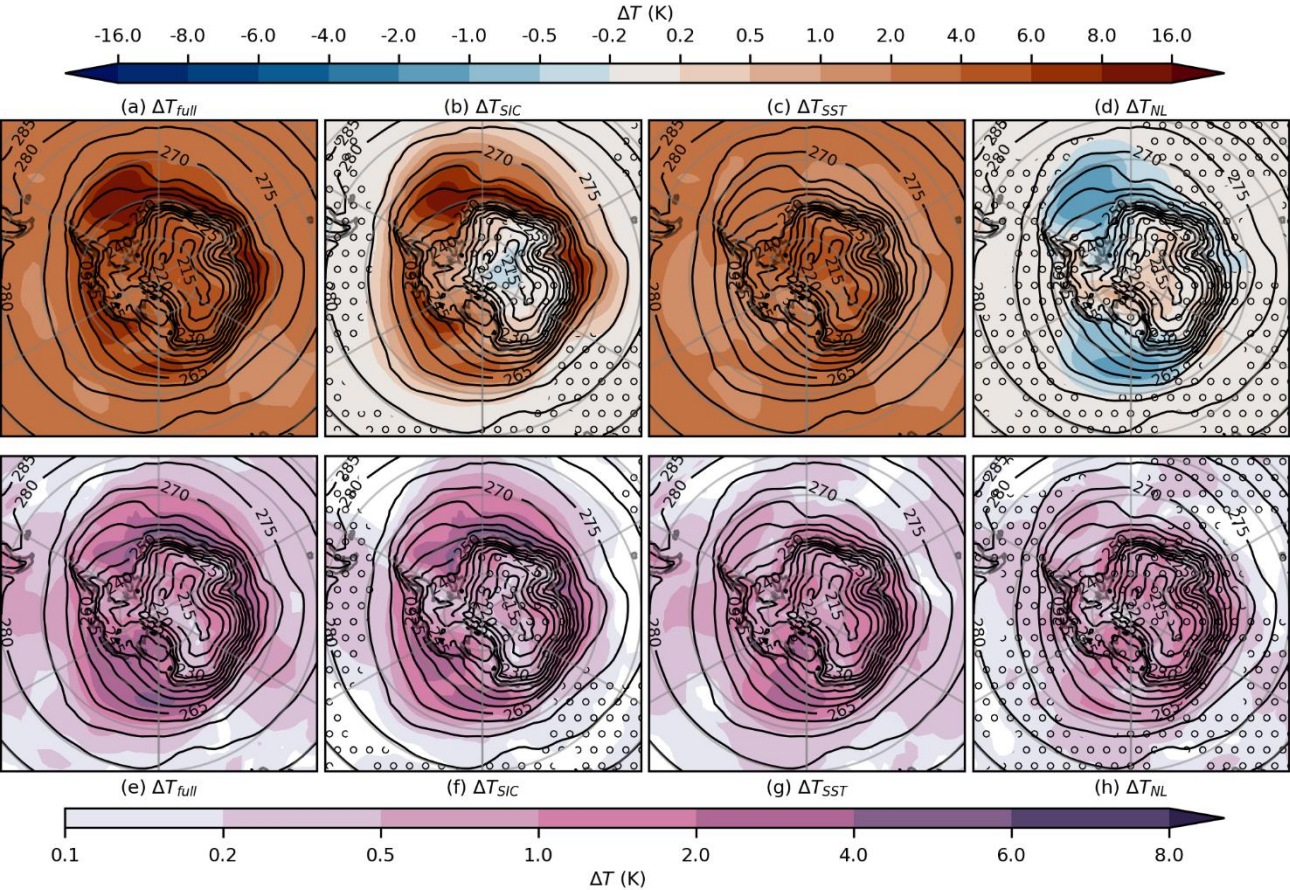
Figure 4. Difference in 2m temperature (T) in austral winter (JJA) between the SSP585 simulation and Baseline (ΔT_{full}, a, e), between SIC_SSP585 and Baseline (ΔT_{SIC}, b, f), between SST_SSP585 and Baseline (ΔT_{SST}, c, g) and the nonlinear (ΔT_{NL} residual) contribution (d, h). The upper row shows the multi-model mean and the lower row the maximum difference between models. Stippling indicates that all models do not agree on the direction of the change and contours show 2m temperature in the Baseline simulation.

The warming over regions that originally had sea ice is predominantly driven by decreases in sea ice cover (ΔT_{SIC}, Fig. 4b) whereas the warming over the continent and ice shelves is mainly caused by warmer SSTs (ΔT_{SST}, Fig. 4c). Over the continent, ΔT_{SIC} is weak or even negative. The difference in 2m temperature between SSP585 and Baseline (ΔT_{full}) is on average close to the sum of the individual changes due to increased SSTs (ΔT_{SST}) and decreased sea ice cover (ΔT_{SIC}), except in the areas where the decrease in sea ice cover causes the largest warming i.e. the Weddell Sea, the D'Urville sea and the Ross Sea (non-stippled ocean regions in Fig. 4h). In these areas, the models agree that the sum of ΔT_{SST} and ΔT_{SIC} is larger than ΔT_{full}. Overall, the models also agree on the warming patterns due to warmer SSTs and decreased sea ice cover.

3.2.2 Mean sea level pressure

The models do not agree on the average change in MSLP ($\Delta MSLP_{full}$) over the Antarctic region: NorESM2 shows a positive $\Delta MSLP_{full}$ on average, EC-Earth3 and OpenIFS show that the average $\Delta MSLP_{full}$ is negative, whereas the average $\Delta MSLP_{full}$ is small in CESM2 (Fig. 3b). All models, except NorESM2, indicate that $\Delta MSLP_{full}$ is on average negative over the southern polar region (Fig. 3b). The multi-model mean $\Delta MSLP_{full}$ is positive over the Pacific sector between 50°S - 70°S and over the Atlantic sector northward of 60°S. In contrast, there is a decrease in MSLP on the Australian side of the Southern Ocean, near the Antarctic coast and over the Weddell Sea (Fig. 5a). However, all models do not agree on the regional pattern of MSLP changes. OpenIFS does not show an increase in MSLP over the Pacific sector, and the maximum decrease in MSLP on the Australian side of the Southern Ocean is also located slightly to the west of the maxima of the other models (Fig. S4). The multi-model mean changes in MSLP indicate a weakening of the Amundsen low while cyclones over the Australian side of the Southern Ocean most likely become deeper or more frequent (or blockings become more infrequent). In addition, a poleward shift of the circumpolar trough, especially in the Atlantic sector, indicates a more positive southern annular mode (SAM) which suggests stronger westerly winds at mid-latitudes and more cyclones near the Antarctic coast.
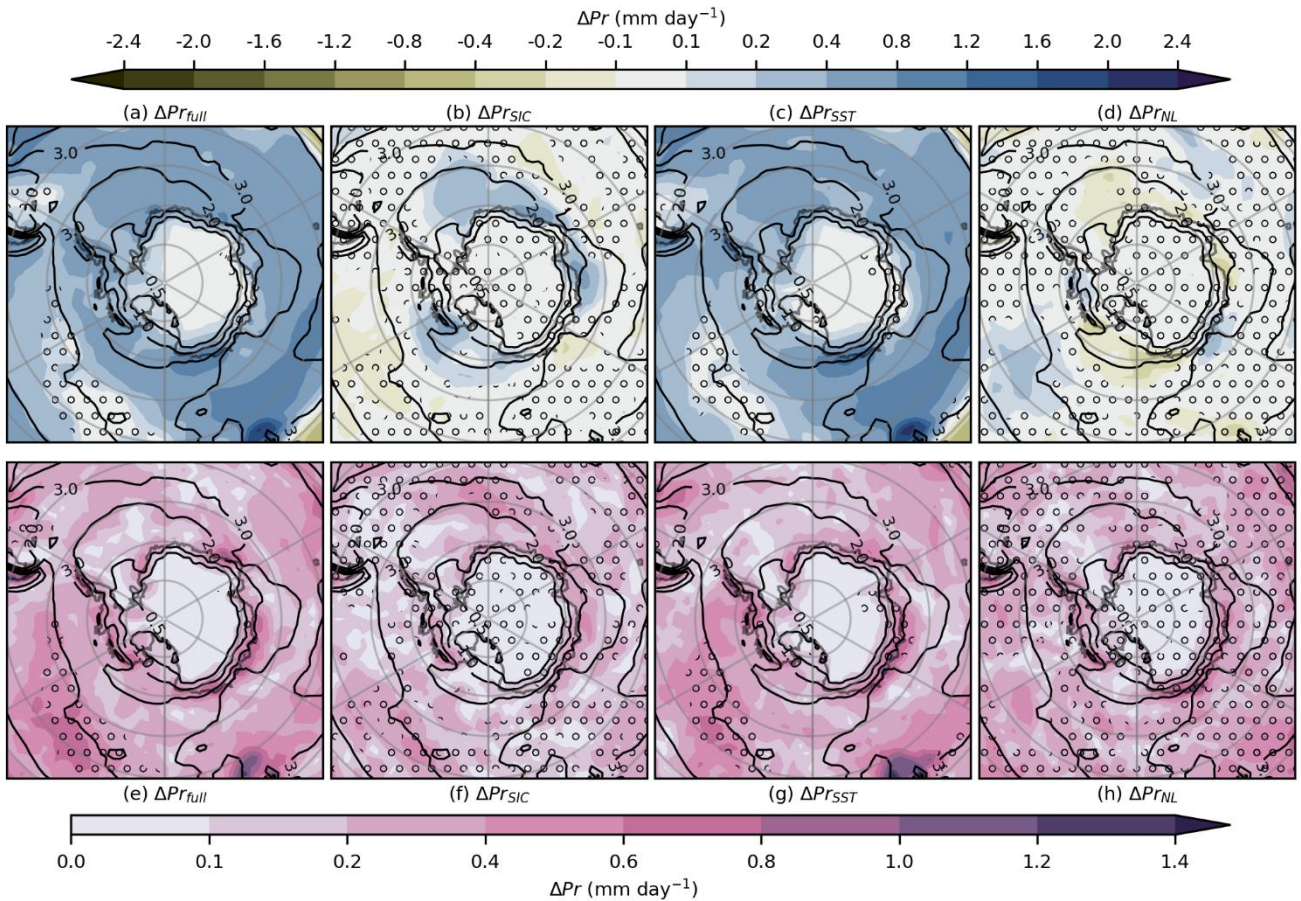
Figure 5. Difference in mean sea level pressure (MSLP) in austral winter (JJA) between the SSP585 simulation and Baseline (ΔMSLP$_{full}$, a, e), between SIC_SSP585 and Baseline (ΔMSLP$_{SIC}$, b, f), between SST_SSP585 and Baseline (ΔMSLP$_{SST}$, c, g) and the nonlinear (ΔMSLP$_{NL}$ residual) contribution (d, h). The upper row shows the multi-model mean and the lower row the maximum difference between models. Stippling indicates that all models do not agree on the direction of the change <u>and contours show MSLP in the Baseline simulation</u>.

The changes in MSLP are mostly driven by warmer SSTs (ΔMSLP$_{SST}$, Fig. 5c), while the decrease in sea ice cover (ΔMSLP$_{SIC}$, Fig. 5b) causes a much weaker response. The models mostly disagree on the direction of the change (stippling in Fig. 5b) except over the Weddell Sea where all models indicate a decrease in MSLP, and over the central continent where all models indicate an increase in MSLP. In some regions, the changes in MSLP due to the decrease in sea ice cover are opposite in sign compared to those driven by the SSTs. Even though the models mostly disagree on the direction of the non-linear change in MSLP (ΔMSLP$_{NL}$), they agree that there is a decrease in MSLP in Amundsen Sea and an increase in MSLP in the Pacific sector of the Southern Ocean (Fig. 5d). The multi-model mean of ΔMSLP$_{NL}$ is mainly opposite to the multi-model mean of ΔMSLP$_{full}$ suggesting that the sum of the individual responses to changes in SST and sea-ice cover overestimates the full response.

3.2.3 Precipitation

All models show a general increase in precipitation (ΔPr_{ful}) over the southern polar region (Fig. 3c), with a similar regional pattern in all models (Fig. S5). The largest absolute increase in precipitation occurs over the Southern Ocean, especially in its Australian sector, where the decrease in MSLP is strongest (Fig. 6a). However, the relative increases are larger over the continent and coastal areas, where there is up to twice as much precipitation in SSP585 compared to Baseline (Fig. S6). Three (CESM2, NorESM2 and EC-Earth3) out of four models indicate that the largest relative increase in precipitation occurs over the continent west of the Ross Sea. These models also show negative or very small positive changes in precipitation in the coastal areas between longitudes of the Indian Ocean side of the Antarctic (90°E - 120°E; right-hand side of the figure panels). The dipole structure in the MSLP changes over the Pacific sector (Fig. 5a) is strongest in these models indicating that these changes in precipitation are, at least partly, driven by changes in circulation.

Figure 6. Difference in precipitation (Pr) in austral winter (JJA) between the SSP585 simulation and Baseline (ΔPr_{full}, a, e), between SIC_SSP585 and Baseline (ΔPr_{SIC}, b, f), between SST_SSP585 and Baseline (ΔPr_{SST}, c, g) and the nonlinear (ΔPr_{NL} residual) contribution (d, h). The upper row shows the multi-model mean and the lower row the maximum difference between models.

14

326 **Stippling indicates that all models do not agree on the direction of the change and contours show precipitation in the Baseline**
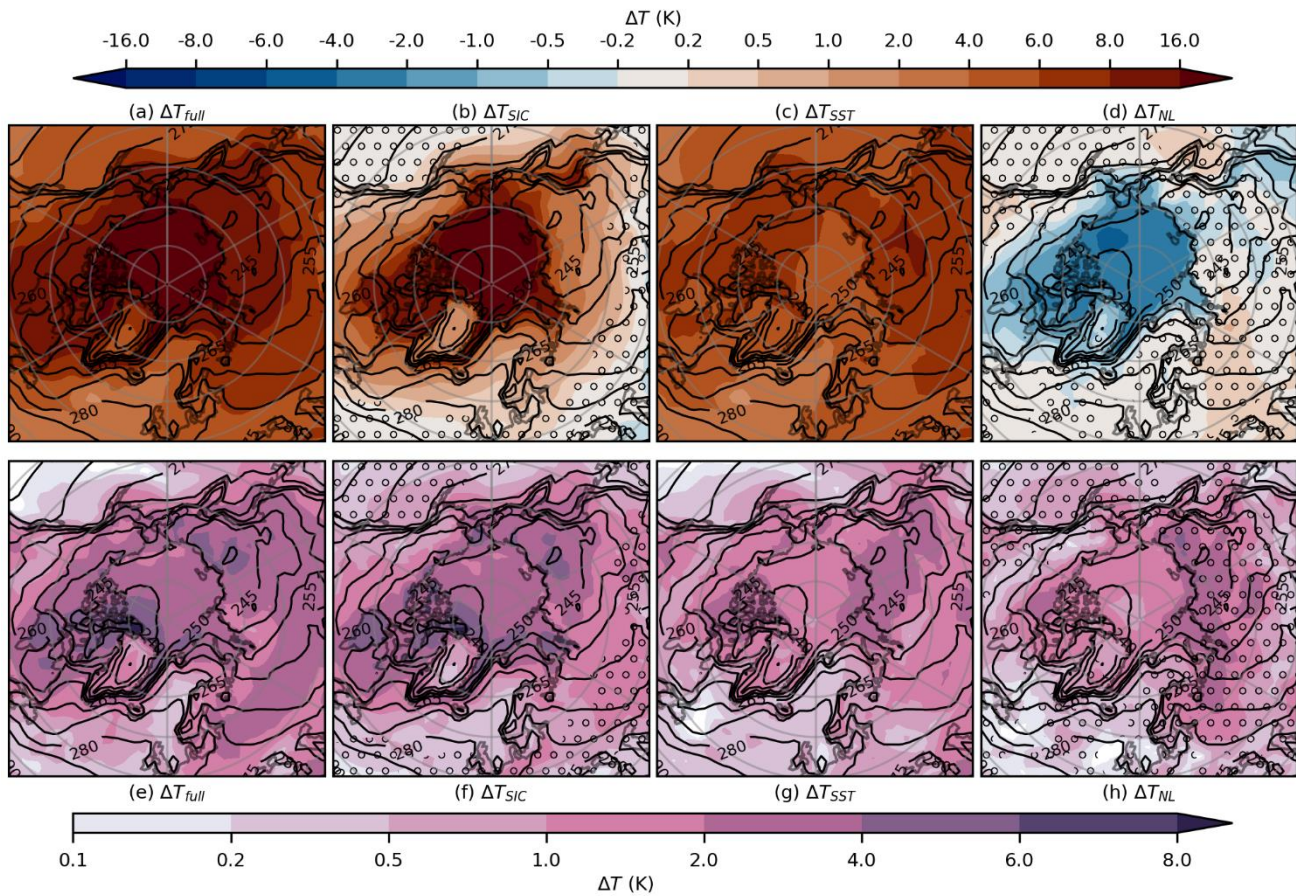327 **simulation.**

328 All models agree that the increase in precipitation is mostly driven by increased SSTs (ΔPr_{SST}, Figs. 3c, 6c) while the decrease

329 in sea ice cover (ΔPr_{SIC}, Fig. 6b) mainly causes small increases in precipitation over the areas where sea ice cover is reduced.

330 The increase in precipitation due to a sea ice decrease (ΔPr_{SIC}) is collocated with the areas where evaporation increases (Fig.

331 S14) suggesting that increased evaporation increases precipitation locally, potentially due to enhanced shallow convection

332 associated with cold air outbreaks. In addition, ΔPr_{SIC} is relatively large over the coastal areas suggesting that enhanced

333 evaporation increases the amount of water vapor in air masses advected to the continent.

334 **3.3 Arctic**

335 **3.3.1 Temperature**

336 In the Arctic, the increase in 2m temperature due to simultaneous changes of SST and sea ice (on average ~13 K) is

337 substantially larger than in the Antarctic (on average ~5 K, Fig. 3a). In the northern hemisphere winter, the largest increases

338 in 2m temperature between SSP585 and Baseline (ΔT_{full}) are found over the Arctic Ocean, Siberia and the Canadian

339 Archipelago (Fig. 7a). All models agree on the general pattern of warming, but there are large absolute differences around

340 northern Greenland, over the Canadian archipelago, and Siberia (Figure 7e). Over Siberia, CESM2 and NorESM2 simulate

341 stronger warming than EC-Earth3 and OpenIFS (Fig. S7). Overall, OpenIFS shows the weakest warming over the continents,

342 whereas NorESM2 shows the strongest warming.

Figure 7. Difference in 2m temperature (T) in winter (DJF) between the SSP585 simulation and Baseline (ΔT_{full}, a, e), between SIC_SSP585 and Baseline (ΔT_{SIC}, b, f), between SST_SSP585 and Baseline (ΔT_{SST}, c, g) and the nonlinear (ΔT_{NL} residual) contribution (d, h). The upper row shows the multi-model mean and the lower row the maximum difference between models. Stippling indicates that all models do not agree on the direction of the change and contours show the 2m temperature in Baseline simulation.

The decrease in sea ice (ΔT_{SIC}, Figs. 3a, 7b) produces on average larger warming than the increase in SSTs (ΔT_{SST}, Fig. 7c) in the northern polar region especially over the Arctic Ocean and in the Canadian archipelago. There, multi-model mean ΔT_{SIC} reaches locally 22 K , which is substantially larger than the maximum ΔT_{SIC} in the Antarctic region (~10 K, Fig. 4b). In general, the decrease in sea ice cover mainly has a local effect on the 2m temperature, i.e. the largest changes occur in the areas or vicinity of the areas where the sea ice cover has decreased, including the coldest areas around the Arctic Ocean, such as Northern Canada and Siberia. The notable increase in 2m temperature over the continents in SIC_SSP585 is most likely due to the different characteristics of the advected air masses from the Arctic Ocean; in Baseline, the Arctic Ocean is ice-covered whereas it is ice-free in SIC_SSP585. The relatively warm air masses do not reach far inland as the strong warming occurs mostly along the coast. Over the other areas of the Arctic, particularly the continents, ΔT_{SST} is larger than ΔT_{SIC}, indicating again that remote effects of SST changes are important for polar continental warming. In areas where both the sea ice decrease

16

359 and the SST increase cause notable warming, i.e. over the Arctic Ocean and in northern Canada, all models indicate a strong

360 non-linearity in the 2m temperature changes, so that the sum of ΔT_{SST} and ΔT_{SIC} is substantially larger than ΔT_{full} (see

361 discussion in Section 4)

3.3.2 Mean sea level pressure

363 The MSLP response to a simultaneous increase in SSTs and a decrease in sea ice cover ($\Delta MSLP_{full}$, Fig. 8a) is more variable

364 between the individual models than the 2m temperature response. All models agree on a MSLP decrease near the Bering Strait

365 suggesting a northward shift and strengthening of the Aleutian low. They also agree that the MSLP decreases in the central

366 Arctic and continental Canada. In contrast, the models disagree on the changes in MSLP over the Atlantic sector. Three out of

367 four models (CESM2, NorESM2 and EC-Earth3) indicate a decrease in MSLP over the Norwegian and Barents Seas,

368 suggesting an eastward extension of the Atlantic storm track, whereas OpenIFS shows an increase in MSLP in the same areas,

369 suggesting a weakening of the Atlantic storm track (Fig. S8).

371
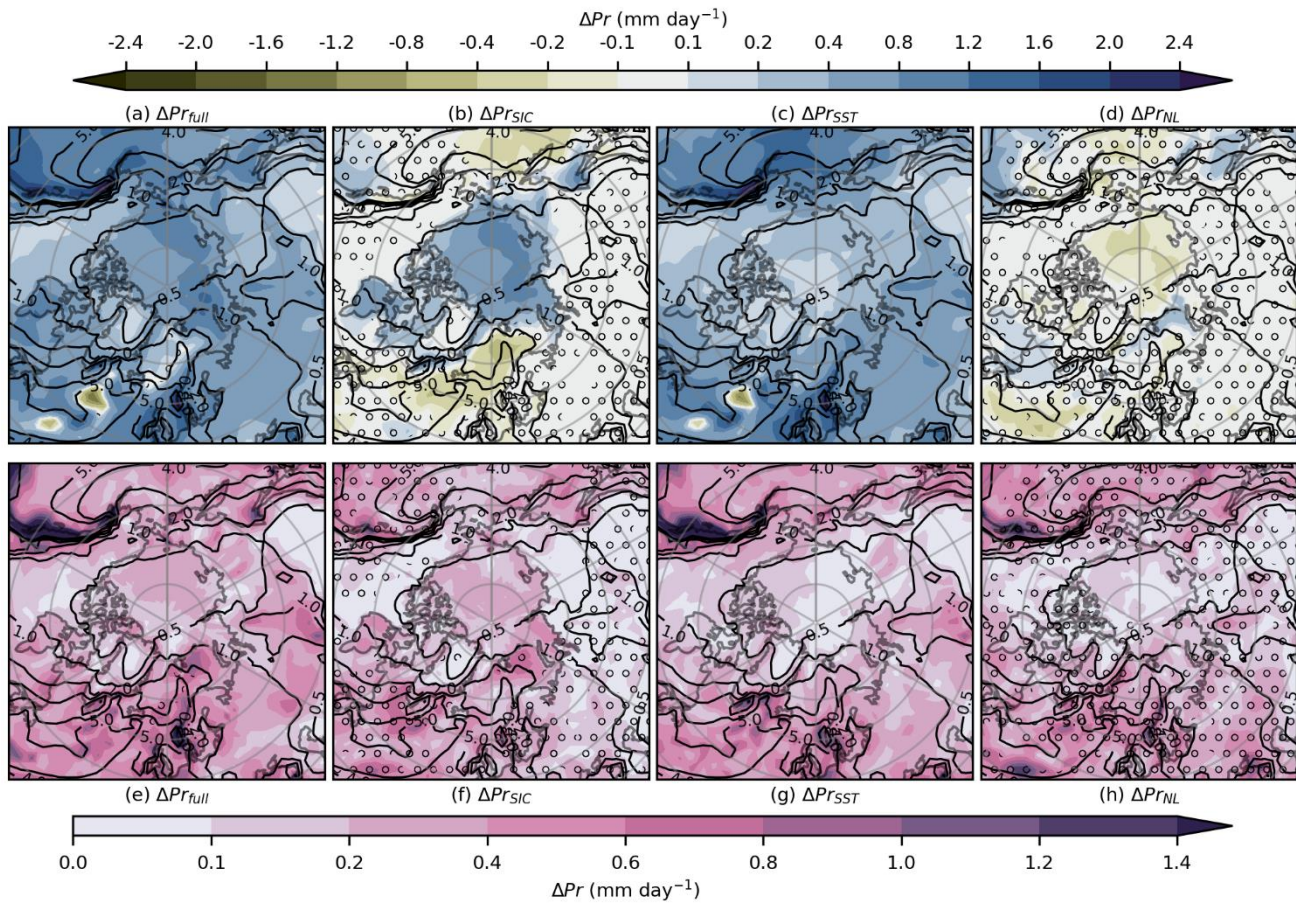
17
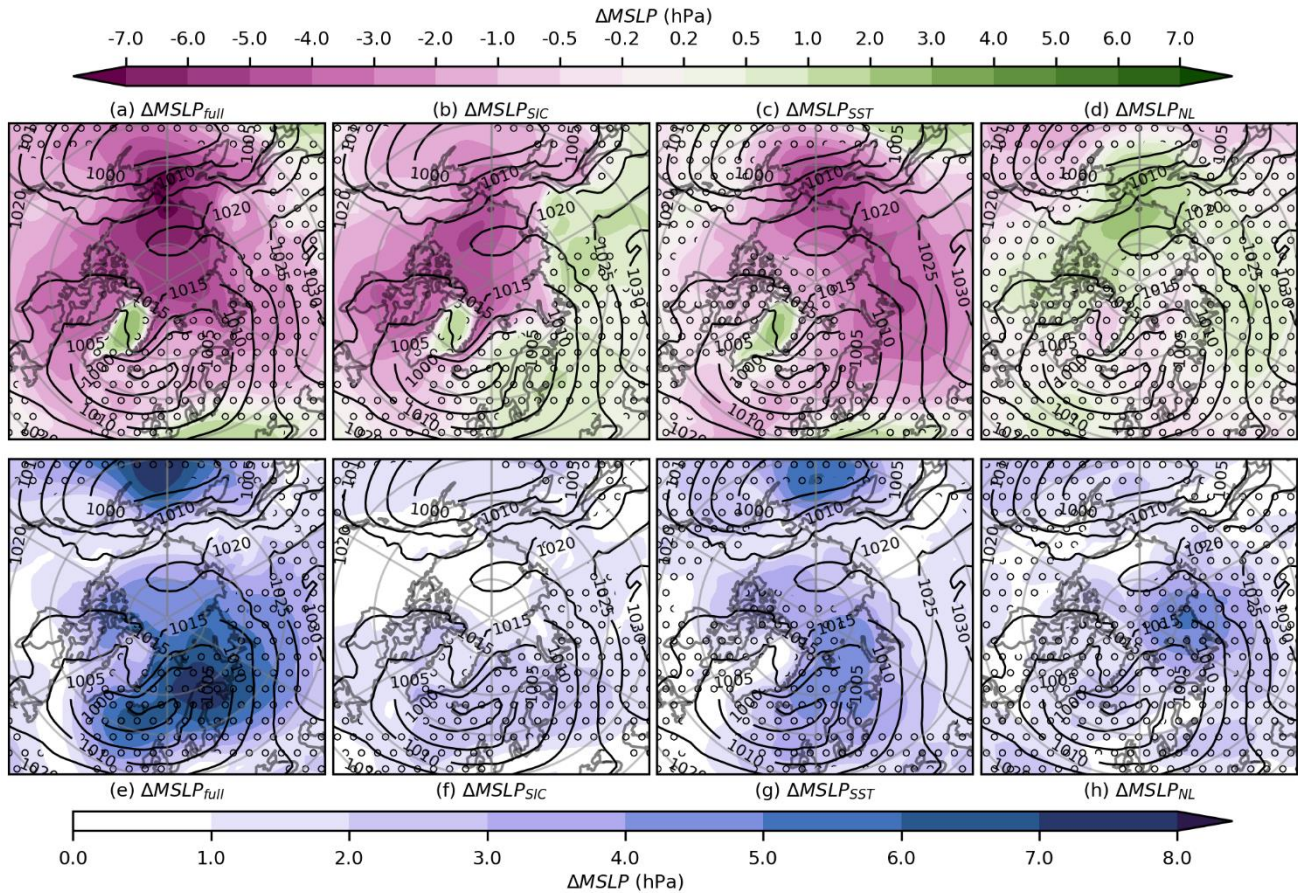
Figure 8. Difference in mean sea level pressure (MSLP) in winter (DJF) between the SSP585 simulation and Baseline (ΔMSLP$_{full}$, a, e), between SIC_SSP585 and Baseline (ΔMSLP$_{SIC}$, b, f), between SST_SSP585 and Baseline (ΔMSLP$_{SST}$, c, g) and the nonlinear (ΔMSLP$_{NL}$ residual) contribution (d, h). The upper row shows the multi-model mean and the lower row the maximum difference between models. Stippling indicates that all models do not agree on the direction of the change and contours show the MSLP in Baseline simulation.

The models agree somewhat better on the MSLP response pattern to individual increases in SST (ΔMSLP$_{SST}$, Fig. 8g) and decreases in sea ice cover (ΔMSLP$_{SST}$, Fig. 8f) than the full response in MSLP (Fig. 8e). In all models,- a decrease in sea ice cover causes a MSLP decrease on the Canadian side of the Arctic Ocean and over the Bering Strait (Fig. 8b). However, the models disagree on the MSLP responses to decreased sea ice cover over Northern Europe, where OpenIFS indicates an increase in MSLP, whereas the other models show only small changes in this region (Fig. S8). Increasing SSTs cause a decrease in MSLP over Siberia, the Siberian side of the Arctic Ocean, and the Bering Strait region in all models. However, over the Northern Atlantic region, the models disagree on the direction of the MSLP changes (Fig. 8g). The non-linearities (ΔMSLP$_{NL}$, Fig. 8d) are typically smaller than the changes due to the individual forcings.

3.3.3 Precipitation

All models agree that the precipitation in the Arctic increases with warmer SSTs and a decrease in sea ice cover (ΔPr$_{full}$, Figs. 3a, 9a). The models also agree on the regional pattern of precipitation change. Most of the precipitation increase is caused by warmer SSTs (ΔPr$_{SST}$, Fig. 9c) and ΔPr$_{SST}$ is larger over the ocean than over land, especially in the areas where the precipitation is strongest climatologically, i.e on the eastern side of the Atlantic and Pacific Oceans. This suggests that the precipitation changes are mainly driven by the increase in atmospheric water vapor content (due to the warmer temperatures that increase the water vapor holding capacity of the air) rather than changes in circulation. In the northern Atlantic, south-east of Greenland, a local decrease in SSTs causes a decrease in precipitation, which also indicates a strong local effect of SST on precipitation. However, the largest relative changes occur in the Arctic Ocean, where the increase in precipitation is at some locations more than twice the original precipitation. Furthermore, over the continents, the relative precipitation increase is larger than over the ocean. Decreasing sea ice cover mainly increases precipitation over the Arctic Ocean. This local response is associated with increased evaporation (Fig. S15), warmer surface air and less stable stratification, which leads to convective precipitation over the Arctic Ocean during cold air outbreaks from continents (not shown). The joint effect of a decrease in sea ice cover and an increase in SST on precipitation is mostly a linear combination of the individual responses and the residuals (ΔPr$_{NL}$, Fig. 9d) are thus mostly small. The models agree the main changes in precipitation i.e. increase in precipitation in the Arctic Ocean due to decrease in sea cover and overall increase in precipitation due to SST increase, however there are quantitative differences between models in increases of precipitation (Figs. 9e-h and S9). Spatially the differences between models are correlated with the strength of precipitation increase.

Figure 9. Difference in precipitation (Pr) in winter (DJF) between the SSP585 simulation and Baseline (ΔPr_{full}, a, e), between SIC_SSP585 and Baseline (ΔPr_{SIC}, b, f), between SST_SSP585 and Baseline (ΔPr_{SST}, c, g) and the nonlinear (ΔPr_{NL} residual) contribution (d, h). The upper row shows the multi-model mean and the lower row the maximum difference between models. Stippling indicates that all models do not agree on the direction of the change and contours show the precipitation in Baseline simulation.

3.4 Effect of surface fluxes

Changes in SST and sea ice cover affect the atmosphere mainly through surface fluxes of sensible and latent heat (Figs. S13, S16). The increase in surface fluxes due to warmer SSTs occurs globally. In fact, the largest increase takes place in the tropics and is driven by surface evaporation. This leads to an increase in atmospheric heat and moisture content also in polar regions through meridional transport, which makes the free troposphere in the polar regions warmer and more moist (Figs. S17, S18). Furthermore, it increases the longwave emission towards the surface. In contrast, a decrease in sea ice cover mainly causes a local, near-surface, climate response in the polar regions. The predominantly strongly stable stratification of the polar troposphere prevents the increased heat and moisture from the surface reaching higher altitudes and thus warming occurs only in the low troposphere of the polar regions (Fig. S17, ΔTSIC). Furthermore, moisture and heat fluxes over the sea equatorward from the original sea ice boundary tend to decrease (Figs. S11, S12, S14, S15, ΔTSIC) because the air masses which are

19

advected equatorward from the areas that were originally covered by sea ice have become warmer and more moist (not shown), which should decrease the temperature and humidity difference between the surface and the advected air mass. On a larger scale, the opposite changes in surface heat and moisture fluxes across the original sea boundary partly balance each other, which reduces the large-scale effect of decreasing sea ice cover.

Over areas where sea ice cover is reduced, our results also show that the sum of the individual effects of decreasing sea cover and increasing SSTs on 2m temperatures is larger than the joint response (Figs. 4, 7). In Baseline, surface heat fluxes are generally negative (downwards) or small over ice-covered areas while they are positive (upwards) over oceans (not shown). When sea ice is removed, surface energy fluxes become positive over areas that used to be ice-covered. The fluxes are slightly higher (more positive) in the simulation where only sea ice cover is reduced (SSP585_SIC, Fig. S11, S12, S14, S15) compared to the joint simulation (SSP585, Fig. S11, S12, S14, S15). The reason is most likely that the air during warm air intrusions (from lower latitudes) and cold air outbreaks (from snow- or ice-covered areas or sea ice) is slightly colder and drier in SSP585_SIC than in SSP585, which enhances the fluxes over the ice-free ocean (where temperatures are set to the freezing point of sea water in both simulations). In the simulation where only SSTs are changed (SSP585_SST, Fig. S11, S12, S14, S15), the surface fluxes become slightly more negative compared to Baseline over areas covered by sea ice. This is probably due to the fact that the air is warmer and more moist during warm air intrusions from lower latitudes, which enhances the energy fluxes towards the surface.

3.5 Comparison between hemispheres

Spatial differences of the responses in meteorological variables between the poles are strongly linked to differences in the geographical environment. In addition, the overall stronger tropospheric warming in the northern hemisphere than in the southern hemisphere due to increased SST (Fig. S17) contributes to a stronger average increase in 2m temperature in the Arctic compared to the Antarctic (Fig. 3a). One factor that contributes to the different responses of meteorological variables between the poles is the overall stronger warming in the northern hemisphere than in the southern hemisphere due to increased SSTs (Fig. S17). However, the differences in the geographical environment also play an important role. In particular, the larger 2m warming in the Arctic as compared to the Antarctic (Fig. 3a) is dominated by the strong near-surface warming due to sea ice loss in the Arctic. The warming is stronger in the Arctic because the original sea ice area is colder in the Arctic than in the Antarctic (Figs. 4 and 7). In addition, in the Arctic, the warming effect caused by a decrease in sea ice cover reaches further in over the continents than in the Antarctic, which may be a consequence of the high surface elevation of the Antarctic ice sheet preventing direct advection of warm near surface air over the continent. A similar but weaker feature is observed over Greenland where the change in 2m temperature due to a sea ice decrease is weaker than in Northern Canada or Siberia.

In both hemispheres, a decrease in sea ice cover causes increases in precipitation over the same area, or the vicinity. Increases in surface latent heat fluxes (Figs S14, S15) and a subsequent weakening of the stable temperature stratification are probably behind this precipitation increase. However, the sea ice decrease has a notably stronger effect on precipitation in the northern polar region than in the southern. SST increases cause a widespread increase in precipitation in both polar regions, but the increase is slightly larger in the Arctic region than in the Antarctic region most likely due to the overall stronger tropospheric warming and moistening in the northern hemisphere (Figs. S17, S18)

In both hemispheres, the uncertainty associated with changes in MSLP is generally larger than the uncertainties associated with changes in 2m temperature and precipitation. In the northern polar region, the decrease in sea ice cover has the largest impact on MSLP, while warmer SSTs dominate the changes in MSLP at the south pole.

4. Discussion

We have used four AGCMs to study the effect of increasing SSTs and decreasing sea ice cover on polar climates. The experimental setup allows us to distinguish the relative contributions of sea ice decreases and SST increases on different climate variables in the polar regions and as well as lower latitudes. A priori, changes in SST and sea ice cover affect the atmosphere mainly through surface fluxes of sensible and latent heat (Figs. S13, S16). The increase in surface fluxes due to warmer SSTs occurs globally. In fact, the largest increase takes place in the tropics and is driven by surface evaporation. This leads to an increase in atmospheric heat and moisture content also in polar regions through meridional transport, which makes the free troposphere in the polar regions warmer and more moist (Figs. S17, S18). Furthermore, it increases the longwave emission towards the surface.

In contrast, a decrease in sea ice cover mainly causes a local, near-surface, climate response in the polar regions. The predominantly strongly stable stratification of the polar troposphere prevents the increased heat and moisture from the surface reaching higher altitudes and thus warming occurs only in the low troposphere of the polar regions (Fig. S17, ΔT_{SIC}). Furthermore, moisture and heat fluxes over the sea equatorward from the original sea ice boundary tend to decrease (Figs. S11, S12, S14, S15, ΔT_{SIC}) because the air masses which are advected equatorward from the areas that were originally covered by sea ice have become warmer and more moist (not shown), which should decrease the temperature and humidity difference between the surface and the advected air mass. On a larger scale, the opposite changes in surface heat and moisture fluxes across the original sea boundary partly balance each other, which reduces the large-scale effect of decreasing sea ice cover. However, our results agree with earlier studies in that sea ice changes dominate the change in 2m temperatures during winter in the area and vicinity of the decreasing sea ice (Screen et al. 2012, Screen and Blackport 2019, Ye et al. 2024).

Over areas where sea ice cover is reduced, our results also show that the sum of the individual effects of decreasing sea cover and increasing SSTs on 2m temperatures is larger than the joint response (Figs. 4, 7). In Baseline, surface heat fluxes are generally negative (downwards) or small over ice-covered areas while they are positive (upwards) over oceans (not shown).

21

481 ~~When sea ice is removed, surface energy fluxes become positive over areas that used to be ice-covered. The fluxes are slightly~~
482 ~~higher (more positive) in the simulation where only sea ice cover is reduced (SSP585_SIC, Fig. S11, S12, S14, S15) compared~~
483 ~~to the joint simulation (SSP585, Fig. S11, S12, S14, S15). The reason is most likely that the air during warm air intrusions~~
484 ~~(from lower latitudes) and cold air outbreaks (from snow- or ice-covered areas or sea ice) is slightly colder and drier in~~
485 ~~SSP585_SIC than in SSP585, which enhances the fluxes over the ice-free ocean (where temperatures are set to the freezing~~
486 ~~point of sea water in both simulations). In the simulation where only SSTs are changed (SSP585_SST, Fig. S11, S12, S14,~~
487 ~~S15), the surface fluxes become slightly more negative compared to Baseline over areas covered by sea ice. This is probably~~
488 ~~due to the fact that the air is warmer and more moist during warm air intrusions from lower latitudes, which enhances the~~
489 ~~energy fluxes towards the surface.~~

490 As sea ice is removed, the insulating layer between the sea water and atmosphere vanishes, which causes a large increase in
491 surface heat fluxes leading to a strong local increase in the 2m temperature (Figs. 4, 7). This effect dominates the change in
492 2m temperatures during winter in the area and vicinity of the decreasing sea ice, in agreement with earlier studies (Screen et
493 al. 2012, Screen and Blackport 2019, Ye et al. 2024, Yu et al. 2024). In contrast, warmer SSTs have a larger effect on 2m
494 temperatures than a reduction of sea ice over the polar continents, which supports the results by Yu et al. (2024). In particular,
495 in the inner Antarctic, the near-surface warming is strongly associated with the remote increase in SSTs. In contrast, the
496 decrease in sea ice cover causes only small or even negative changes in 2m temperature over the inner continent, most likely
497 due to a weak advection of near surface-air from the ocean to the inner continent. Furthermore, at both poles, the SST increase
498 causes mostly stronger 2m temperature increases over the continents than over the ocean due to the overall tropospheric
499 warming and increasing downwelling longwave radiation, which in turn is strongly driven by increased moisture in the
500 troposphere and a higher tropospheric temperature, due to an increase in latent heat release. Overall, the effects of SST increase
501 and sea ice decrease on 2m temperature are linearly additive. However, the sum of the individual effects of decreasing sea
502 cover and increasing SSTs on 2m temperatures is sometimes larger than the joint response over areas where sea ice cover is
503 reduced

504 In agreement with earlier studies (e.g. Screen and Blackport 2019, Streffing et al 2021), we find that the uncertainty in the
505 dynamical response (MSLP) is larger than in the thermodynamic response. However, the models in our study do agree on
506 many features of the MSLP pattern changes, e.g. decreases in MSLP in the central Arctic and in the D'Urville Sea in the
507 Antarctic. Previous sStudies ~~focusing on the effect of Arctic sea ice decrease on MSLP~~ (Yu et al. 2024, Ye et al. 2024, Smith
508 et al. 2022; Chripko et al.,2021; Screen et al., 2018; Deser et al., 2010) have shown that reduced Arctic sea ice cover tend to
509 increases the MSLP over the Northern Atlantic. while it decreases over ~~They have also shown increasing MSLP in~~ Siberia and
510 ~~decreasing MSLP in the~~ the Aleutian region. These results generally agree with our SSP585_SIC experiment , although some
511 of the details in the pattern of the MSLP response differ. ~~However, warmer SSTs cause a larger and opposite effect on MSLP~~
512 ~~in the Northern Atlantic region leading to an overall decrease in MSLP when both sea ice cover and SST changes are~~

513 ~~considered.~~ In particular, our multi-model mean response only shows an increase in MSLP over the Scandinavian side of the
514 northern Atlantic while the MSLP decreases over the Icelandic region and the western northern Atlantic. It is worth noting,
515 however, that the models in our study do not agree on the direction of the MSLP response over the northern Atlantic, meaning
516 that there is a large uncertainty. Furthermore, in particular over the northern Atlantic, warmer SSTs generally produce a larger
517 MSLP response than a decrease in sea ice cover in our simulations. Our multi-model mean results are produced from a 4
518 model×40 years ensemble. Despite the many years of simulation this may not be enough to capture the entire internal variability
519 associated with dynamical variables such as MSLP, in particular in terms of their response to sea ice cover changes (Peings et
520 al. 2021 and Sun et al. 2022). Our ensemble is produced by four models, which should capture a larger part of the internal
521 climate variability compared to an ensemble generated by only one model. However, our ensemble only represents two model
522 families meaning that the results are more dependent on each other than four completely independent models.

523 The precipitation response includes a thermodynamic response (increase in water vapor content), a local dynamic response
524 (changes in e.g. convection) and a large-scale dynamic response (changes in e.g. storm tracks). Our simulations show that
525 warmer SSTs generally increase precipitation in the polar regions mainly due to the overall increase in atmospheric water
526 vapor content (Fig. S18). Decreasing sea ice cover, on the other hand, mainly increases precipitation in areas where sea cover
527 is reduced, indicating that enhanced local evaporation and convection during cold air outbreaks is the main cause of
528 precipitation changes. In general, this result is in agreement with previous studies (Yu et al. 2023, 2024) and can be linked to
529 the high warming scenario (SSP5-8.5) where thermodynamic and local effects are expected to dominate over large-scale
530 dynamic effects in terms of changes in precipitation (Yu et al. 2023, 2024). ~~This suggests that thermodynamic and local effects~~
531 ~~dominate over large scale dynamic effects in terms of changes in precipitation. However, this result may be related to our~~
532 ~~experimental setup, where we use a high warming scenario (SSP5-8.5) to generate sea ice and SST forcing files. Such a high~~
533 ~~warming scenario will generate a large increase in atmospheric water vapor which may overshadow the dynamical effects~~
534 ~~which have shown to be more important e.g. in the PAMIP experiments (Yu et al. 2023).~~

5. Conclusions and perspectives

536 We have used four AGCMs to examine the climate response in the polar regions and lower latitudes to prescribed future global
537 changes in SST and sea ice cover, with a focus on wintertime 2m temperatures, MSLP, and surface precipitation at high
538 latitudes.Generally, the models agree on the response in 2m temperature and surface precipitation, in particular in terms of the
539 spatial distribution and the relative impact of warming SSTs and decreasing sea ice cover. The models agree less well on the
540 magnitude and spatial distribution of the MSLP response, i.e. the uncertainties associated with the atmospheric circulation
541 response are larger than the uncertainties associated with the thermodynamic response. The models agree on an increase in
542 MSLP in the central Arctic and Bering strait as well as in the D'Urville sea in the Antarctic but disagree on the changes over
543 Northern Europe and the Northern Atlantic.

23

Changing sea ice cover and SSTs cause about the same average warming poleward of 60°N/S in winter, whereas warmer SSTs increase precipitation more strongly than decreasing sea ice cover. This result applies to both poles and implies that a ~~major~~ substantial part of the polar near-surface warming and precipitation increase is a response to remote SST forcing. Furthermore, increasing SSTs cause an overall larger tropospheric warming and moistening of the northern hemisphere, which contributes to stronger increases in precipitation and 2m temperature in the Arctic than in the Antarctic. The MSLP response to changing SSTs tends to be of approximately similar magnitude (Arctic) or larger (Antarctic) than the response to changing sea ice cover - and the responses sometimes counteract each other. Warmer SSTs also have a wide-spread impact on 2m temperatures and precipitation, while a decrease in sea ice cover mainly causes a localized response, i.e. the warming and increased precipitation tend to occur in the areas (or in the vicinity of the areas) where the sea ice disappears. The reason for this localized response is most likely the strong temperature stratification in the polar regions in winter, which prevents the increased surface heat fluxes from affecting higher levels of the atmosphere. Thus, a decrease in sea ice cover produces a weak effect on the thermodynamic variables outside the areas of sea ice retreat. SST changes dominate the polar 2m temperature and precipitation responses outside the areas of sea ice retreat, including the Antarctic continent.

The models predict that the change in 2m temperature and precipitation at both poles is generally linear, i.e. the modelled response to simultaneous changes in SSTs and sea ice is approximately equal to the sum of the individual changes. The main exceptions are the areas within and in the vicinity of the zone of sea ice retreat. Over these areas, the sum of the individual responses in 2m temperature and precipitation to decreasing sea ice cover and increasing SSTs is larger than the joint effect. This result suggests that some of the polar warming that is caused by warmer SSTs outside the polar regions (and subsequent increased-large scale heat and moisture transport) weakens the contribution of surface turbulent fluxes to polar warming, i.e. the remote response weakens the local response.

At both poles, o~~O~~ur results show that the largest uncertainty in the climate response to decreases in sea ice cover and warmer SSTs is associated with atmospheric circulation, as the largest differences between the models was found for MSLP. Note that these discrepancies occurred even though the models were constrained by the same oceanic boundary conditions. The circulation response to decreasing sea ice cover was sometimes enhanced but sometimes also counteracted by the response to warmer SSTs. This finding is particularly important to consider when drawing conclusions about changes in mid-latitude circulation to changing sea ice cover using either observations or model simulations where the two effects (from decreasing sea ice and changing SSTs) cannot easily be separated. Furthermore, to decrease the uncertainty and improve our confidence in climate predictions it is important to disentangle the causes behind the differences in the circulation responses between the models. The model setup and output presented here are unique in this aspect and can be used to explore the underlying physical processes.

Data availability

CESM2: https://archive.sigma2.no/pages/public/datasetDetail.jsf?id=10.11582/2024.00018 and monthly mean values are available: https://crices-task33-output-cesm2-monthly-means.lake.fmi.fi/index.html

NorESM2: https://doi.org/10.17043/naakka-2025-noresm2-1 and monthly mean values are available: https://crices-task33-output-noresm-monthly-means.lake.fmi.fi/index.html ~~At the moment NorESM2 data is available from the authors upon request and it will be published~~

EC-Earth3: https://crices-task33-output-ecearth.lake.fmi.fi/index.html and

https://crices-task33-output-ecearth-ifs-monthly-means.lake.fmi.fi/index.html

~~https://crices-task33-output-ecearth-ifs-monthly-means.lake.fmi.fi/index.html~~

OpenIFS: https://a3s.fi/CRiceS_Index/CRiceS_index.html. and monthly mean values are available: https://crices-task33-output-openifs-monthly-means.lake.fmi.fi/index.html ~~At the moment OpenIFS data is available from the authors upon request and it will be published~~

Code availability

CESM2: documentation is available at https://escomp.github.io/CESM/versions/cesm2.2/html/: The code is available at: https://github.com/ESCOMP/CESM

NorESM2: Documentation is available at https://www.noresm.org/. The code is available at: https://github.com/NorESMhub/NorESM

EC-Earth3: Brief general documentation of EC-Earth3 is provided at https://ec-earth.org/ec-earth/ec-earth3/. See also the papers by Döscher et al. (2022) and van Noije et al. (2021). The code is available to registered users at https://ec-earth.org/ec-earth/ec-earth-development-portal/. Only employees of institutes that are part of the EC-Earth consortium can obtain an account.

OpenIFS: Documentation is available at https://confluence.ecmwf.int/display/OIFS. The licence for using the OpenIFS model can be requested from ECMWF user support (openifs-support@ecmwf.int).

Authors contributions

Planning the study: TN, DK, KN, PR, MTL, RM, JM, BHS, VAS, JLT, AMLE

Running experiments: TN, DK, KN, PR

Analysing results: TN, DK, KN, PR with support by MTL, RM, JM, BHS, VAS, JLT, AMLE

Writing manuscript: TN, DK, PR and AE with input and support from KN, MTL, RM, JM, BHS, VAS, JLT

Competing interests

604   The authors declare that they have no conflict of interest.

605

621

622   **References**

623   Balsamo, G., Beljaars, A., Scipal, K., Viterbo, P., van den Hurk, B., Hirschi, M., and Betts A. K.: A revised hydrology for the
624   ECMWF model: Verification from field site to terrestrial water storage and impact in the Integrated Forecast System, Journal
625   of hydrometeorology, 10, 3, 623-643, doi:10.1175/2008JHM1068.1, 2009

626   Bozzo, A., Remy, S., Benedetti, A., Flemming, J., Bechtold, P., Rodwell, M. J., and Morcrette, J. J.: Implementation of a
627   CAMS-based aerosol climatology in the IFS, Technical memorandum Vol. 801, 1-33 Reading, UK: European Centre for
628   Medium-Range Weather Forecasts. doi:10.21957/84ya94mls, 2017

629   Chripko, S., Msadek, R., Sanchez-Gomez, E., Terray, L., Bessières, L., and Moine, M. P.: Impact of reduced arctic sea ice on
630   northern hemisphere climate and weather in autumn and winter. Journal of Climate, 34, 14, 5847-5867, doi: 10.1175/JCLI-D-
631   20-0515.1, 2021

Cohen, J., Screen, J. A., Furtado, J. C., Barlow, M., Whittleston, D., Coumou, D., Francis, J., Dethloff, K., Entekhabi, D., Overland, J. and Jones, J.: Recent Arctic amplification and extreme mid-latitude weather. Nature geoscience, 7, 9, 627-637, doi:10.1038/ngeo2234, 2014

Cronin, T. W., Li, H., and Tziperman, E.: Suppression of Arctic air formation with climate warming: Investigation with a two-dimensional cloud-resolving model, Journal of the Atmospheric Sciences, 74, 9, 2717-2736, doi:10.1175/JAS-D-16-0193.1, 2017

Danabasoglu, G., Lamarque, J. F., Bacmeister, J., Bailey, D. A., DuVivier, A. K., Edwards, J., Emmons, L. K., Fasullo, J., Garcia, R., Gettelman, A., and Hannay, C., The community earth system model version 2 (CESM2). Journal of Advances in Modeling Earth Systems, 12, 2, p.e2019MS00191, doi:10.1029/2019MS001916, 2020

Deser, C., Tomas, R., Alexander, M., and Lawrence, D.: The seasonal atmospheric response to projected Arctic sea ice loss in the late twenty-first century. Journal of Climate, 23, 2, 333-351, doi: 10.1175/2009JCLI3053.1, 2010

Döscher, R., Acosta, M., Alessandri, A., Anthoni, P., Arsouze, T., Bergman, T., Bernardello, R., Boussetta, S., Caron, L.-P., Carver, G., Castrillo, M., Catalano, F., Cvijanovic, I., Davini, P., Dekker, E., Doblas-Reyes, F. J., Docquier, D., Echevarria, P., Fladrich, U., Fuentes-Franco, R., Gröger, M., v. Hardenberg, J., Hieronymus, J., Karami, M. P., Keskinen, J.-P., Koenigk, T., Makkonen, R., Massonnet, F., Ménégoz, M., Miller, P. A., Moreno-Chamarro, E., Nieradzik, L., van Noije, T., Nolan, P., O'Donnell, D., Ollinaho, P., van den Oord, G., Ortega, P., Prims, O. T., Ramos, A., Reerink, T., Rousset, C., Ruprich-Robert, Y., Le Sager, P., Schmith, T., Schrödner, R., Serva, F., Sicardi, V., Sloth Madsen, M., Smith, B., Tian, T., Tourigny, E., Uotila, P., Vancoppenolle, M., Wang, S., Wårlind, D., Willén, U., Wyser, K., Yang, S., Yepes-Arbós, X., and Zhang, Q.: The EC-Earth3 Earth system model for the Coupled Model Intercomparison Project 6, Geosci. Model Dev., 15, 2973–3020, https://doi.org/10.5194/gmd-15-2973-2022, 2022.

ECMWF, Surface Parametrization, IFS documentation CY40R1 Part IV: Physical Processes ECMWF 111-113: Reading, UK, doi:10.21957/f56vvey1x, 2014

England, M.R., Polvani, L.M., Sun, L. and Deser, C.: Tropical climate responses to projected Arctic and Antarctic sea-ice loss. Nature Geoscience, 13, 4, 275-281, doi:10.1038/s41561-020-0546-9, 2020

Gates, W. L.: AMIP: The Atmospheric Model Intercomparison Project. Bull. Amer. Meteor. Soc., 73, 1962–1970, 10.1175/1520-0477(1992)073,1962:ATAMIP.2.0.CO;2, 1992

Gates, W. L., Boyle, J. S., Covey, C., Dease, C. G., Doutriaux, C. M., Drach, R. S., Fiorino, M., Gleckler, P. J., Hnilo, J. J., Marlais, S. M. and Phillips, T. J.: An overview of the results of the Atmospheric Model Intercomparison Project (AMIP I). Bull. Amer. Meteor. Soc., 80, 29–55, 10.1175/1520-0477(1999)080,0029:AOOTRO.2.0.CO;2, 1999

Gettelman A, and Morrison H.: Advanced two-moment bulk microphysics for global models. Part I: Off-line tests and comparison with other schemes. Journal of Climate. 28, 3, 1268-87, doi:10.1175/JCLI-D-14-00102.1, 2015

Gettelman, A., Liu, X., Ghan, S. J., Morrison, H., Park, S., Conley, A .J., Klein, S. A., Boyle, J., Mitchell, D. L. and Li, J. L.: Global simulations of ice nucleation and ice supersaturation with an improved cloud scheme in the Community Atmosphere Model, Journal of Geophysical Research: Atmospheres, 115, D18, doi:10.1029/2009JD013797, 2010

Han, J. S., Park, H. S. and Chung, E. S.: Projections of central Arctic summer sea surface temperatures in CMIP6. Environmental Research Letters, 18, 12, 124047, doi:10.1088/1748-9326/ad0c8a, 2023

Hogan, R. J., and Bozzo, A.: A flexible and efficient radiation scheme for the ECMWF model. Journal of Advances in Modeling Earth Systems, 10, 8, 1990-2008, doi:10.1029/2018MS001364, 2018

IPCC, 2022: Climate Change 2022: Impacts, Adaptation and Vulnerability. Contribution of Working Group II to the Sixth Assessment Report of the Intergovernmental Panel on Climate Change [H.-O. Pörtner, D.C. Roberts, M. Tignor, E.S. Poloczanska, K. Mintenbeck, A. Alegría, M. Craig, S. Langsdorf, S. Löschke, V. Möller, A. Okem, B. Rama (eds.)]. Cambridge University Press. Cambridge University Press, Cambridge, UK and New York, NY, USA, 3056 pp., doi:10.1017/9781009325844

Kim H. M. and Kim B. M.: Relative Contributions of Atmospheric Energy Transport and Sea Ice Loss to the Recent Warm Arctic Winter Journal of Climate 30, 18, 7441-7450, doi:10.1175/JCLI-D-17-0157.1, 2018

Kirkevåg, A., Iversen, T., Seland, Ø., Hoose, C., Kristjánsson, J. E., Struthers, H., Ekman, A. M. L., Ghan, S., Griesfeller, J., Nilsson, E. D., and Schulz, M.: Aerosol–climate interactions in the Norwegian Earth System Model – NorESM1-M, Geoscientific Model Development, 6, 207–244, doi:10.5194/gmd-6-207-2013, 2013

Kirkevåg, A., Grini, A., Olivié, D., Seland, Ø., Alterskjær, K., Hummel, M., Karset, I. H. H., Lewinschal, A., Liu, X., Makkonen, R., Bethke, I., Griesfeller, J., Schulz, M., and Iversen, T.: A production-tagged aerosol module for Earth system models, OsloAero5. 3–extensions and updates for CAM5.3-Oslo. Geoscientific Model Development, 11, 10, 3945-3982, doi:10.5194/gmd-11-3945-2018, 2018

Kittel, C., Amory, C., Hofer, S., Agosta, C., Jourdain, N. C., Gilbert, E., Le Toumelin, L., Vignon, É., Gallée, H., and Fettweis, X.: Clouds drive differences in future surface melt over the Antarctic ice shelves, The Cryosphere, 16, 2655–2669, doi:10.5194/tc-16-2655-2022, 2022.

Lenaerts, J. T., Van Tricht, K., Lhermitte, S. and L'Ecuyer, T. S.: Polar clouds and radiation in satellite observations, reanalyses, and climate models, Geophysical Research Letters, 44, 7, 3355-3364 doi:10.1002/2016GL072242, 2017

Liu, X., Ma, P.-L., Wang, H., Tilmes, S., Singh, B., Easter, R. C., Ghan, S. J., and Rasch, P. J.: Description and evaluation of a new four-mode version of the Modal Aerosol Module (MAM4) within version 5.3 of the Community Atmosphere Model, Geoscientific Model Development, 9, 505–522, doi:10.5194/gmd-9-505-2016, 2016.

Morcrette, J., Barker, H. W., Cole, J. N. S., Iacono, M. J. and Pincus, R.: Impact of a new radiation package, McRad, in the ECMWF Integrated Forecasting System, Monthly Weather Review, 136, 4773–4798, doi:10.1175/2008MWR2363.1, 2008

van Noije, T. P. C., Le Sager, P., Segers, A. J., van Velthoven, P. F. J., Krol, M. C., Hazeleger, W., Williams, A. G., and Chambers, S. D.: Simulation of tropospheric chemistry and aerosols with the climate model EC-Earth, Geoscientific Model Development., 7, 2435–2475, doi:10.5194/gmd-7-2435-2014, 2014.

van Noije, T., Bergman, T., Le Sager, P., O'Donnell, D., Makkonen, R., Gonçalves-Ageitos, M., Döscher, R., Fladrich, U., von Hardenberg, J., Keskinen, J.-P., Korhonen, H., Laakso, A., Myriokefalitakis, S., Ollinaho, P., Pérez García-Pando, C., Reerink, T., Schrödner, R., Wyser, K., and Yang, S.: EC-Earth3-AerChem: a global climate model with interactive aerosols and atmospheric chemistry participating in CMIP6 , Geoscientific Model Development, 14, 5637–5668, doi:10.5194/gmd-14-5637-2021, 2021.

Notz, D., and SIMIP Community: Arctic sea ice in CMIP6. Geophysical Research Letters,47, e2019GL086749, doi:10.1029/2019GL086749, 2020

Parkinson, C. L.: Arctic sea ice coverage from 43 years of satellite passive-microwave observations. Frontiers in Remote Sensing, 3, 1021781, doi:10.3389/frsen.2022.1021781, 2022

Parkinson, C. L.: A 40-y record reveals gradual Antarctic sea ice increases followed by decreases at rates far exceeding the rates seen in the Arctic. Proceedings of the National Academy of Sciences, 116, 29, 14414-14423. doi.org/10.1073/pnas.1906556116, 2019

Peings, Y., Labe, Z. M., and Magnusdottir, G.: Are 100 ensemble members enough to capture the remote atmospheric response to +2°C Arctic sea ice loss? Journal of Climate, *34,* 10, 3751–3769, doi:10.1175/jcli-d-20-0613.1, 2021

Rantanen, M., Karpechko, A.Y., Lipponen, A., Nordling, K., Hyvärinen, O., Ruosteenoja, K., Vihma, T. and Laaksonen, A.: The Arctic has warmed nearly four times faster than the globe since 1979. Communications earth & environment, 3, 1, 168, doi:10.1038/s43247-022-00498-3, 2022

Ryan, J. C., Smith, L. C., Cooley, S. W., Pearson, B., Wever, N., Keenan, E. and Lenaerts, J. T. M.: Decreasing surface albedo signifies a growing importance of clouds for Greenland Ice Sheet meltwater production, Nature Communications, *13*, 1, 4205, doi:10.1038/s41467-022-31434-w, 2022

Screen, J. A., and Simmonds, I.: Increasing fall-winter energy loss from the Arctic Ocean and its role in Arctic temperature amplification. Geophysical research letters, 37, 16, doi:10.1029/2010GL044136, 2010

Screen, J. A., and Blackport, R.: How robust is the atmospheric response to projected Arctic sea ice loss across climate models? Geophysical Research Letters, 46, 20, 11406-11415, doi:10.1029/2019GL084936, 2019

Screen, J. A., Deser, C., and Simmonds, I.: Local and remote controls on observed Arctic warming, Geophysical Research Letters, 39, 10, doi:10.1029/2012GL051598, 2012

Screen, J. A., Deser, C., Smith, D. M., Zhang, X., Blackport, R., Kushner, P. J., Oudar, T., McCusker, K. E. and Sun, L.: Consistency and discrepancy in the atmospheric response to Arctic sea-ice loss across climate models. Nature Geoscience, 11, 3, 155-163, doi:10.1038/s41561-018-0059-y, 2018

Seland, Ø., Bentsen, M., Olivié, D., Toniazzo, T., Gjermundsen, A., Graff, L. S., Debernard, J. B., Gupta, A. K., He, Y.-C., Kirkevåg, A., Schwinger, J., Tjiputra, J., Aas, K. S., Bethke, I., Fan, Y., Griesfeller, J., Grini, A., Guo, C., Ilicak, M., Karset, I. H. H., Landgren, O., Liakka, J., Moseid, K. O., Nummelin, A., Spensberger, C., Tang, H., Zhang, Z., Heinze, C., Iversen, T., and Schulz, M.: Overview of the Norwegian Earth System Model (NorESM2) and key climate response of CMIP6 DECK, historical, and scenario simulations, Geoscientific Model Development, 13, 6165–6200, doi:10.5194/gmd-13-6165-2020, 2020.

Smith, D. M., Screen, J. A., Deser, C., Cohen, J., Fyfe, J. C., García-Serrano, J., Jung, T., Kattsov, V., Matei, D., Msadek, R., Peings, Y., Sigmond, M., Ukita, J., Yoon, J.-H., and Zhang, X.: The Polar Amplification Model Intercomparison Project (PAMIP) contribution to CMIP6: investigating the causes and consequences of polar amplification, Geoscientific Model Development, 12, 1139–1164, doi:10.5194/gmd-12-1139-2019, 2019

Smith, D.M., Eade, R., Andrews, M. B., Ayres, H., Clark, A., Chripko, S., Deser, C., Dunstone, N. J., García-Serrano, J., Gastineau, G. Graff, L. S. Hardiman, S. C., He, B., Hermanson, L., Jung, T., Knight, J., Levine, X., Magnusdottir, G., Manzini, E., Matei, D., Mori, M., Msadek, R., Ortega, P., Peings, Y., Scaife, A. A., Screen, J. A., Seabrook, M., Semmler, T., Sigmond,

M., Streffing, J., Sun, L. and Walsh, A.: Robust but weak winter atmospheric circulation response to future Arctic sea ice loss. Nature communications, 13, 1, 727, doi: 10.1038/s41467-022-28283-y, 2022

Storelvmo, T., Kristjánsson, J. E., Ghan, S. J., Kirkevåg, A., Seland, Ø., and Iversen, T.: Predicting cloud droplet number concentration in Community Atmosphere Model (CAM)-Oslo. Journal of Geophysical Research: Atmospheres, 111, D24, doi:10.1029/2005JD006300, 2006

Streffing, J., Semmler, T., Zampieri, L., and Jung, T.: Response of Northern Hemisphere weather and climate to Arctic sea ice decline: Resolution independence in Polar Amplification Model Intercomparison Project (PAMIP) simulations. Journal of Climate, 34, 20, 8445-8457, doi:10.1175/JCLI-D-19-1005.1, 2021

Stuecker, M. F., Bitz, C. M., Armour, K. C., Proistosescu, C., Kang, S. M., Xie, S. P., Kim, D., McGregor, S., Zhang, W., Zhao, S. and Cai, W.: Polar amplification dominated by local forcing and feedbacks, Nature Climate Change 8, 12, 1076-1081 doi: 10.1038/s41558-018-0339-y, 2018

Sun, L., Deser, C., Simpson, I., and Sigmond, M.: Uncertainty in the winter tropospheric response to Arctic Sea ice loss: The role of stratospheric polar vortex internal variability. Journal of Climate, 35, 10, 3109–3130, doi:10.1175/jcli-d-21-0543.1, 2022

Tewari, K., Mishra, S. K., Salunke, P., Ozawa, H., and Dewan, A.: Potential effects of the projected Antarctic sea-ice loss on the climate system. Climate Dynamics, 60, 1, 589-601, doi:10.1007/s00382-022-06320-2, 2023

Vihma, T.: Effects of Arctic Sea Ice Decline on Weather and Climate: A Review. Surveys in Geophysics, 35, 1175–1214 doi:10.1007/s10712-014-9284-0, 2014

Wendisch, M., Macke, A., Ehrlich, A., Lüpkes, C., Mech, M., Chechin, D., Dethloff, K., Velasco, C.B., Bozem, H., Brückner, M. … and Zeppenfeld, S.: The Arctic cloud puzzle: Using ACLOUD/PASCAL multiplatform observations to unravel the role of clouds and aerosol particles in Arctic amplification, Bulletin of the American Meteorological Society, 100, 5, 841-871, doi: 10.1175/BAMS-D-18-0072.1, 2019

Ye, K., Woollings, T., Sparrow, S. N., Watson, P. A., and Screen, J. A.: Response of winter climate and extreme weather to projected Arctic sea-ice loss in very large-ensemble climate model simulations, npj Climate and Atmospheric Science, 7, 1, 20, doi: 10.1038/s41612-023-00562-5, 2024

Yu, H., Screen, J. A., Hay, S., Catto, J. L., and Xu, M.: Winter Precipitation Responses to Projected Arctic Sea Ice Loss and Global Ocean Warming and Their Opposing Influences over the Northeast Atlantic Region, Journal of Climate, 36(15), 4951-4966, doi: 10.1175/JCLI-D-22-0774.1, 2023

Yu, H., J. A. Screen, M. Xu, S. Hay, and J. L. Catto: Comparing the Atmospheric Responses to Reduced Arctic Sea Ice, a Warmer Ocean, and Increased CO_2 and Their Contributions to Projected Change at 2°C Global Warming. Journal of Climate, 37, 23, 6367–6380, doi:10.1175/JCLI-D-24-0104.1, 2024

Ziehn, T., Chamberlain, M., Lenton, A., Law, R., Bodman, R., Dix, M., Wang, Y., Dobrohotoff, P., Srbinovsky, J., Stevens, L., Vohralik, P., Mackallah, C., Sullivan, A., O'Farrell, S., and Druken, K.: 2019 CSIRO ACCESS-ESM1.5 model output prepared for CMIP6 CMIP historical. Version 20191128. Earth System Grid Federation, doi:10.22033/ESGF/CMIP6.4272, 2019a

Ziehn, T., Chamberlain, M., Lenton, A., Law, R., Bodman, R., Dix, M., Wang, Y., Dobrohotoff, P., Srbinovsky, J., Stevens, L., Vohralik, P., Mackallah, C., Sullivan, A., O'Farrell, S., and Druken, K.: 2019 CSIRO ACCESS-ESM1.5 model output prepared for CMIP6 ScenarioMIP ssp585. Version 20191128. Earth System Grid Federation, doi:10.22033/ESGF/CMIP6.4333, 2019

Ziehn, T., Chamberlain, M. A., Law, R. M., Lenton, A., Bodman, R. W., Dix, M., Stevens, L., Wang, Y. P. and Srbinovsky, J.: The Australian Earth System Model: ACCESS-ESM1.5, Journal of Southern Hemisphere Earth Systems Science, 70, 1, 193-214. doi:10.1071/ES19035, 2020